



Below Average Midsummer to Early Autumn Precipitation Evolved Into the Main Driver of Sudden Scots Pine Vitality Decline in the Swiss Rhône Valley

Stefan Hunziker^{1*}, Michael Begert², Simon C. Scherrer², Andreas Rigling^{1,3} and Arthur Gessler^{1,3}

¹ Research Unit Forest Dynamics, Swiss Federal Institute for Forest, Snow and Landscape Research WSL, Birmensdorf, Switzerland, ² Climate Division, Federal Office of Meteorology and Climatology MeteoSwiss, Zurich, Switzerland, ³ Institute of Terrestrial Ecosystems, ETH Zurich, Zurich, Switzerland

OPEN ACCESS

Edited by:

Rüdiger Grote,
Karlsruhe Institute of Technology
(KIT), Germany

Reviewed by:

Jesús Julio Camarero,
Spanish National Research Council
(CSIC), Spain

Maxime Cailleret,
Institut National de Recherche pour
l'Agriculture, l'Alimentation et
l'Environnement (INRAE), France

*Correspondence:

Stefan Hunziker
stefan.hunziker@wsl.ch

Specialty section:

This article was submitted to
Forests and the Atmosphere,
a section of the journal
Frontiers in Forests and Global
Change

Received: 11 February 2022

Accepted: 28 April 2022

Published: 13 June 2022

Citation:

Hunziker S, Begert M,
Scherrer SC, Rigling A and Gessler A
(2022) Below Average Midsummer
to Early Autumn Precipitation Evolved
Into the Main Driver of Sudden Scots
Pine Vitality Decline in the Swiss
Rhône Valley.
Front. For. Glob. Change 5:874100.
doi: 10.3389/ffgc.2022.874100

The vitality of Scots pine (*Pinus sylvestris* L.) is declining since the 1990s in many European regions. This was mostly attributed to the occurrence of hotter droughts, other climatic changes and secondary biotic stressors. However, it is still not well understood which specific atmospheric trends and extremes caused the observed spatio-temporal dieback patterns. In the Swiss Rhône valley, we identified negative precipitation anomalies between midsummer and early autumn as the main driver of sudden vitality decline and dieback events. Whereas climate change from 1981 to 2018 did not lead to a reduced water input within this time of the year, the potential evapotranspiration strongly increased in spring and summer. This prolonged and intensified the period of low soil moisture between midsummer and autumn, making Scots pines critically dependent on substantial precipitation events which temporarily reduce the increased water stress. Thus, local climate characteristics (namely midsummer to early autumn precipitation minima) are decisive for the spatial occurrence of vitality decline events, as the lowest minima outline the most affected regions within the Swiss Rhône valley. Mortality events will most likely spread to larger areas and accelerate the decline of Scots pines at lower elevations, whereas higher altitudes may remain suitable Scots pine habitats. The results from our regional study are relevant on larger geographic scales because the same processes seem to play a key role in other European regions increasingly affected by Scots pine dieback events.

Keywords: *Pinus sylvestris* L., forest dieback, tree mortality, crown defoliation, climate change, heat drought, reference evapotranspiration, soil drought

INTRODUCTION

Climate change affects ecosystems all over the world. The frequency and intensity of droughts (especially hotter droughts with higher vapor pressure deficits) and pest outbreaks increased in many regions, which affected tree vitality and often resulted in widespread tree mortality (Allen et al., 2010, 2015; Park Williams et al., 2013; Hartmann et al., 2018; Schuldt et al., 2020). Therefore,

forest dieback has become one of the predominant climate change impact on plants and ecosystems (Breshears et al., 2018).

Within these global changes, the vitality of Scots pines (*Pinus sylvestris* L.) declined in various regions across Europe (Vilà-Cabrera et al., 2013; Bose et al., 2020; Senf et al., 2020). In dry inner-Alpine valleys, a large number of trees have been subject to mortality events in the last decades (e.g., Cech and Perny, 2000; Pfister et al., 2001; Gonthier et al., 2010; Vacchiano et al., 2012) and several such events occurred in the Swiss Rhône valley (e.g., Rebetez and Dobbertin, 2004; Bigler et al., 2006; Rigling et al., 2018). Specific events were, however, limited to certain areas at lower altitude (Dobbertin, 2005; Rigling et al., 2006, 2013; Etzold et al., 2019). The Scots pine decline started in the 1990s, and most of the aforementioned studies identified increased drought stress as the main responsible factor. This coincides with the exceptionally high magnitude of climatic changes on the global scale since the 1980s (IPCC, 2014; Reid et al., 2016). However, the relative importance of changing climate parameters such as atmospheric water demand vs. precipitation on forest decline patterns is still poorly understood and hampers the ability to anticipate future climate change impacts (Park Williams et al., 2013; Grossiord et al., 2020). For instance, Rigling et al. (2018) demonstrated a connection between multi-annual periods of a strongly negative climatic water balance and Scots pine vitality drops and dieback. This correlation, however, is not very consistent, does not apply to several single years, and the magnitudes of negative climatic water balance anomalies do not match the magnitudes of tree vitality decline. Similar results were found for the correlation between the April to August climatic water balance and subsequent annual mortality rates (Rigling et al., 2013).

Besides drought stress, various further factors may affect Scots pine vitality and mortality. Infestations by insects, pathogens, nematodes, and the hemi-parasite mistletoe (*Viscum album*) may increase tree mortality (e.g., Dobbertin and Rigling, 2006; Rigling et al., 2006; Dobbertin et al., 2007; Wermelinger et al., 2008; Pastirčáková et al., 2018; Taccoen et al., 2019) especially when trees have been predisposed by drought stress. Plant competition (Weber et al., 2007; Archambeau et al., 2020) and non-drought related climatic extreme events such as spring frost or extreme heat (Teskey et al., 2015; Vitasse and Rebetez, 2018; Vitasse et al., 2018) may act as additional factors reducing the vitality of Scots pines. Finally, the long-term cumulative impact of all site specific predisposing, initiating and contributing factors (Manion, 1991) was found to be decisive for Scots pine mortality (e.g., Rigling and Cherubini, 1999; Bigler et al., 2006; Camarero et al., 2015). Due to this complexity, it is difficult to disentangle the respective effects of particular climatic change factors and other potential stressors (Dale et al., 2001; Taccoen et al., 2019).

The present study aims to (1) identify the main climatic drivers of sudden Scots pine vitality decline and dieback on an annual time scale, (2) analyze temporal changes of climatic parameters responsible for the increased occurrence of vitality decline and dieback events since the 1990s, and (3) explain the pronounced spatial differences of the observed

forest dieback. The Swiss Rhône valley is an ideal test field to address these research questions because Scots pines were monitored on several forest plots since the 1990s and a dense meteorological station network provides long-term and high-quality climate data. As tree vitality cannot be measured directly (Dobbertin, 2005), we used observations of the tree crown defoliation as vitality indicator (Innes, 1998; Eickenscheidt and Wellbrock, 2014) and the often strongly related (particularly for co-dominant and dominant trees) mortality as the ultimate indicator of non-vitality (Dobbertin and Brang, 2001; Rigling et al., 2018). We analyzed and combined data of vitality observations with further parameters of forest observations, climatic changes and anomalies since 1981 including further data sources such as soil water measurements and remote sensing in order to disentangle the effects of climate parameters and other impact factors. In a further step, we tested the main finding on cases of dieback events in other European regions and we drew conclusions on the likely future development of the Scots pine population within the study area.

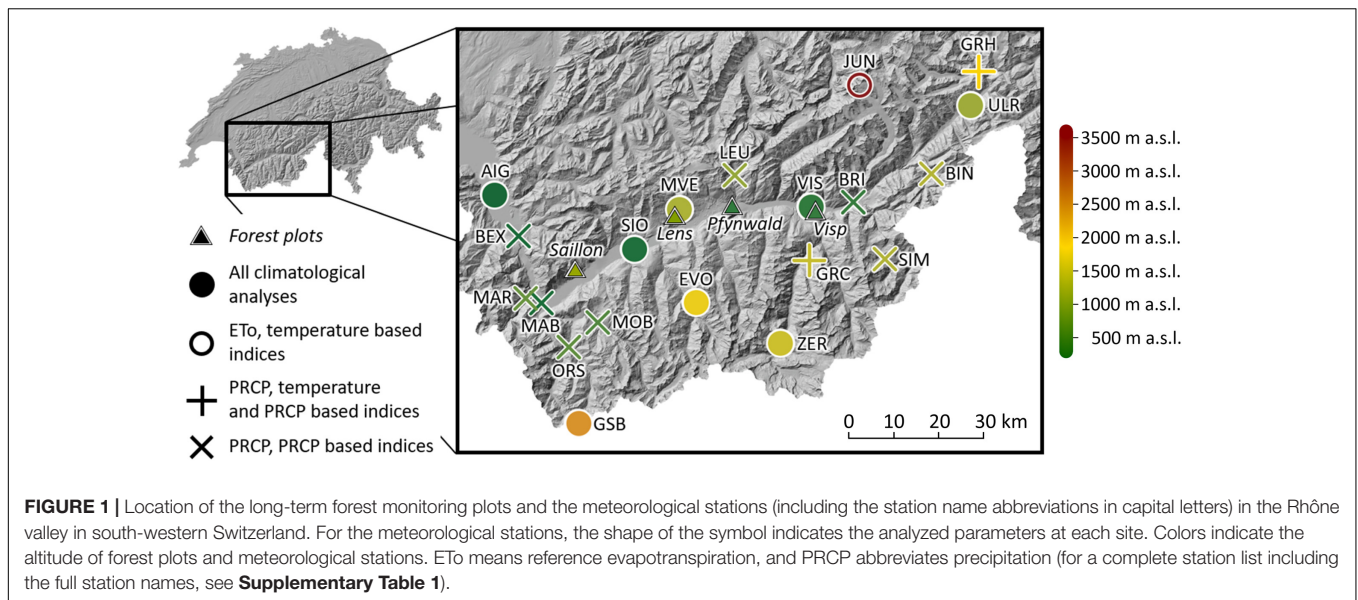
MATERIALS AND METHODS

Study Area

The Swiss Rhône valley is a dry inner-Alpine valley located in south-western Switzerland (**Figure 1**). Long-term annual mean precipitation (1981–2018) is lowest in the central part of the valley with a minimum of 594 mm in Sion (abbreviated SIO). The regional annual mean temperature maximum (1981–2018) is reached at the same site with 10.8°C.

Scots pine is a common tree species in the Rhône valley which is dominant on the monitored forest plots near Visp (0.5 ha, 695 meters above sea level (m a.s.l.), 46°18'N, 7°52'E), in Pfywald (0.4 ha, 615 m a.s.l., 46°18'N, 7°37'E), near Saillon (0.05 ha, 1,192 m a.s.l., 46°10'N, 7°09'E), and near Lens (0.5 ha, 1,063 m a.s.l., 46°16'N, 7°26'E). All the forest plots were unmanaged. During the analyzed time periods (Visp and Saillon: 1996–2018, Pfywald: 2003–2018, Lens: 2005–2018), the average stand densities of living trees per ha (all trees with diameters at breast height ≥ 12 cm were monitored) were 171 (Visp), 680 (Pfywald), 739 (Saillon), and 992 (Lens). The corresponding basal areas were 5 m²/ha (Visp), 24 m²/ha (Pfywald), 42 m²/ha (Saillon) and 35 m²/ha (Lens). Besides Scots pine, further tree species found on the forest plot near Visp were whitebeam (*Sorbus aria*, 27% of the living trees) and pubescent oak (*Quercus pubescens*, 10% of the living trees). On the forest plot near Saillon, 20% of the trees were spruce (*Picea abies*) and 27% beech (*Fagus sylvatica*). On the forest plots in Pfywald and near Lens, other tree species were limited to a few single individuals.

The mean diameters at breast height of the Scots pines analyzed within this study were 20 cm (Visp and Pfywald), 39 cm (Saillon) and 25 cm (Lens). The vast majority of these Scots pines were co-dominant or dominant trees (i.e., they reached or rose above the average canopy top). The average



defoliation of living Scots pines on the forest plots was 24% (Visp), 35% (Pfywald), 27% (Saillon) and 25% (Lens). A medium or strong mistletoe infestation (i.e., low infestation at several parts of the tree crown, strong infestation at single parts of the crown, or strong infestation at several crown parts) was observed on 11% (Visp), 46% (Pfywald) and 13% (Lens) of the Scots pines.

Soils in the Rhône valley are predominantly weakly developed and shallow with a low water-retention capacity. The soils on the forest plots were classified as Pararendzinas near Visp and in Pfywald and as Cambisols near Saillon and Lens (Etzold et al., 2018, personal communication with Stephan Zimmermann).

Forest Observations

Visual estimation of tree crown defoliation (i.e., the proportion of needles or leaves that should be present on a tree but which have been lost) is a key indicator and the most commonly used index for tree health (Innes, 1998; Eickenscheidt and Wellbrock, 2014). It is evaluated regardless the cause of foliage loss, so it includes, for example, damage by insects (Eichhorn and Roskams, 2013). Besides defoliation, crown condition assessments include various further parameters and are done annually within the Swiss Long-term Forest Ecosystem monitoring network (LWF, see Innes, 1995; Dobbertin, 2005; Schönbeck et al., 2018) and follow the protocols of the ICP Forests program.¹ Tree crown defoliation is quantified in 5% steps from 0% (i.e., completely healthy) to 100% (i.e., dead). Previous studies identified about three quarters of individual tree crown defoliation assessments to be within $\pm 5\%$ from the observer mean or control team (Eickenscheidt and Wellbrock, 2014; Ferretti et al., 2014). Internal (LWF) and international (ICP Forests) training and calibration courses indicate that observations by the LWF field experts assessing crown defoliation in the Swiss Rhône valley were well within

this error margin. Within ICP Forests, the total amount of defoliation is estimated, but LWF field experts additionally record the amount of defoliation of unknown reasons, which is the remaining defoliation after subtracting the amount of defoliation caused by obvious reasons. This allows the identification and damage quantification of certain disturbances such as insect infestations. Other impacts such as previous frost events may not be recognized, however, if the damages are unspecific at the time of the assessment.

Even though the forest plots analyzed in the present study were initiated with different aims [the plots near Visp and Lens are ICP Forests Level II plots, the plot near Saillon is a Level I plot, and the plot in Pfywald is an experimental plot (see Joseph et al., 2020) of which only the unmanipulated control-subplots were considered], the observations were taken by the same field experts complying the same protocol. However, the different plot types affected the average Scots pine sample sizes on the plots, which are 47 near Visp, 270 in Pfywald, 18 near Saillon and 8 near Lens. Only time series with annual resolution were considered, which strongly reduced the tree number in Lens because inventories were mostly iterating between two subplots. Newly ingrown trees with a diameter at breast height ≥ 12 cm were included every few years in the sample of the forest plots. Volumetric soil water content was monitored continuously at the site near Visp since 2009 in 15, 50, and 80 cm soil depth using soil moisture sensors (ECH2O EC-5; Decagon Devices). Large fractions of missing values between 2009 and 2012 limited the period of analyzable soil water measurements to 2013–2018.

To corroborate potential frost damage on the forest plot near Visp, multispectral satellite data of Planet Labs PBC² with a 3.7 m image resolution were analyzed. Color infrared (CIR) imagery is suitable to detect the amount of chlorophyll in the plant tissue and hence estimate the health condition of Scots

¹<http://icp-forests.net/page/icp-forests-manual>

²<https://www.planet.com>

pine foliage and other vegetation (Fassnacht et al., 2012; Masaitis et al., 2013) before and after a potentially damaging event. CIR images were created by changing the band combination as follows: red = Near Infrared band, green = red band and blue = green band.

Defoliation Change and Mortality

Forest observations were quality controlled by detecting and removing erroneous data and internal inconsistencies. For assessing the temporal development of tree vitality, we calculated time series of annual defoliation changes. Namely, we calculated the defoliation change ($D_{\text{Change}(j)}$) on the forest plots for each time step j by averaging the annual defoliation changes of the individual trees:

$$D_{\text{Change}(j)} = \frac{1}{n} \sum_{i=1}^n (D_{i(j)} - D_{i(j-1)})$$

where n is the number of Scots pines on the plot, $D_{i(j)}$ the defoliation of tree i in year j , and $D_{i(j-1)}$ the defoliation of tree i in the previous year.

Defoliation change time series are much more robust against temporal inconsistencies of the sample than time series of the simple mean defoliation. For example, mean defoliation time series often indicate a recovery of tree crowns after a mortality event. This may be a false conclusion and just caused by the exclusion of dead trees (i.e., 100% defoliated trees). Furthermore, trees with a higher defoliation are more likely to die during a stress phase, which may result in a shift toward less defoliation in the sample composition. Hence, the mean defoliation may poorly represent actual mean crown defoliation trajectories.

In the present study, we were interested in mortality related to and impacts impairing tree health. Certain events, such as severe storms, rockfalls, or forest management interventions, may result in the removal of trees irrespective of their vitality. Such cases may therefore, disturb the correlation between tree vitality, mortality and stress impacts. Furthermore, it is important to keep the relationship between defoliation and mortality coherent. Therefore, we applied restrictions to defoliation time series and defined tree mortality as follows:

- Mortality of a tree was stated when the defoliation reached 100% (observation must be corroborated in the subsequent crown assessment).
- Mortality was furthermore attributed to trees that were fallen or degraded due to natural causes (i.e., no human interventions) and that were defoliated by $\geq 80\%$ in the previous year.
- In rare cases, trees may seem completely defoliated while being still alive. Therefore, if a defoliation of 100% was reported followed by a defoliation estimation $< 100\%$ in the next assessment, the defoliation value of 100% was replaced by 95%.
- In order to determine the exact mortality year of individual trees, only defoliation time series containing measurements in the year before mortality were considered.

- Defoliation time series that stopped because of other reasons than mortality as defined above were not considered.
- Trees with more than one missing defoliation observation in the last 2 years of the analyzed time period were not considered.

Climate Observations

Time series of the atmospheric variables from the Swiss Rhône valley were generated by the Federal Office of Meteorology and Climatology (MeteoSwiss). In order to get comprehensive and reliable information on climatic changes and extremes in the study area, 20 meteorological stations (**Figure 1**) with a data completeness $\geq 84\%$ between 1981 and 2018 were analyzed. The period 1981–2018 was chosen for trend analyses in order to cover the shift of the climate regime in the 1980s (Reid et al., 2016) and hence potentially important changes just before the occurrence of Scots pine mortality events in the 1990s.

Station elevations range from 381 to 3,580 m a.s.l. The station at 3,580 m a.s.l. is located clearly above the tree line (up to ca. 2,500 m a.s.l.), but it contributes to the assessment of the elevation dependence of the climatic trend signals relevant for the target mortality areas at lower altitudes. A detailed list of the stations, data availability and completeness is provided in **Supplementary Table 1**.

We used data on a monthly time scale of the atmospheric variables maximum temperature, minimum temperature, vapor pressure, sunshine duration, wind speed, and precipitation (PRCP). Note that for most analyses, we transformed vapor pressure to relative humidity (Allen et al., 1998) in order to remove temperature dependence from the humidity measure. For the calculation of climate change indices, daily maximum and minimum temperature and PRCP data were used. All time series were quality controlled and homogenized by MeteoSwiss (Begert et al., 2005). Rarely occurring missing values in the monthly time series were interpolated from neighboring stations using linear regression models (Frei and Schär, 1998; Frei, 2014) and, in case of missing daily PRCP data, from a computer mapping algorithm (Frei et al., 2006). Since the present study focuses on trends, particular emphasis was placed upon selecting atmospheric variables that were least exposed to temporal inhomogeneities. For instance, we used sunshine duration for the calculation of the reference evapotranspiration and not direct radiation measurements because the latter were more affected by instrument changes. As a consequence, sunshine duration had to be transformed to net radiation (Allen et al., 1998).

The spatial analysis of mild extremes of low midsummer to early autumn PRCP sums with a 5-year return period is based on the monthly interpolated PRCP dataset of MeteoSwiss (RhiresM), from which the 20th percentile of July to September PRCP sums from 1981 to 2018 were extracted. PRCP time series from 1981 to 2018 for other European regions affected by Scots pine mortality events were derived from the

interpolated E-OBS dataset with a grid resolution of 0.25° (Haylock et al., 2008).

All analyses were done on annual and seasonal time scales. For the seasons, winter includes the months December of the previous year to February (DJF), spring March to May (MAM), summer June to August (JJA), and autumn September to November (SON). For some analyses, further time periods were analyzed such as midsummer to early autumn (July to September) or the estimated vegetation period (April to September).

Reference Evapotranspiration and Vapor Pressure Deficit

Evapotranspiration describes the water transfer from vegetation and soil to the atmosphere and reaches some two-thirds of the average PRCP amount over the entire land surface (Baumgartner and Reichel, 1975). The actual evapotranspiration can be adequately estimated by calculating the potential evapotranspiration from standard atmospheric measurements (e.g., Sumner and Jacobs, 2005; Calanca et al., 2011). For this, we used the approach of the Food and Agriculture Organization of the United Nations which calculates the reference evapotranspiration (ET_o) (Allen et al., 1998). It is one of the more physically sound methods (Hargreaves and Allen, 2003) and it is widely used in various research fields (Ortega-Farias et al., 2009; Sentelhas et al., 2010; Amatya and Harrison, 2016). The approach is based on the Penman-Monteith method (Penman, 1948; Monteith, 1965) and requires atmospheric measurements of temperature, humidity, sunshine, and wind speed. In the context of a changing climate, methods that include these four key variables should be preferred over methods taking into account less input parameters (McMahon et al., 2013). Further details on the calculation of the ET_o and considerations regarding its adequacy over forest stands can be found in **Supplementary Text 1**.

To identify drivers of ET_o trend signals, we performed sensitivity analyses and calculated ET_o time series with only one atmospheric variable as driver while keeping the other variables constant. In other words, to quantify the impact of temperature, temperature measurements were used together with 1981–2018 means of relative humidity, sunshine duration, and wind speed to calculate the ET_o. Any trend signal and variability in the resulting ET_o time series reflect consequently the specific impact of temperature. ET_o trend signals calculated with different variables as drivers can be compared directly. Furthermore, we quantified the impact of the atmospheric variables on ET_o variability and extremes. This was done by calculating the centered root mean squared fraction and converting it to a percentual efficiency measure (see **Supplementary Text 2 for details**).

The vapor pressure deficit (VPD) is the difference between the saturation vapor pressure and the actual vapor pressure (Seager et al., 2015) and depends therefore on the atmospheric variables temperature and humidity. It is one of the critical parameters driving evapotranspiration (Castellví et al., 1996; Allen et al., 1998). Besides its role for the water loss to the

atmosphere, the VPD may directly impact the functioning of trees and affect plant physiology in absence as well as in combination with drought (Grossiord et al., 2020; Trotsiuk et al., 2020; Zweifel et al., 2021). Therefore, it was analyzed in addition to the ET_o.

Climatic Water Balance

The climatic water balance is a simple parameter integrating the main water in- and output by subtracting the ET_o from PRCP. It is often used as indicator for drought and tree water stress (e.g., Eilmann et al., 2011; Rigling et al., 2013; Buras et al., 2020). However, the climatic water balance does not consider various factors that are relevant for site specific water availability such as the (short-term) temporal distribution of PRCP events, runoff, soil water storage capacity, and difference between the potential and actual evapotranspiration. Therefore, we focus on temporal changes and anomalies instead of absolute values of the climatic water balance.

Climate Change Indices

For an in-depth insight into the changes of climatic conditions in the Swiss Rhône valley and to analyze potential impacts of (mild) atmospheric extremes on Scots pines, we computed and analyzed six climate change indices (**Table 1**). These indices are largely based on the definitions by the CCI/CLIVAR/JCOMM Expert Team on Climate Change Detection and Indices (ETCCDI).³ In contrast to the ET_o, the VPD, PRCP, and the climatic water balance, the climate change indices are calculated from daily weather observations and may therefore identify trend signals and extremes which remain undetected by the other parameters.

Trend Estimation, Linear Regression and Correlation

Trends of most atmospheric parameters and indices were calculated with the non-parametric Theil-Sen trend estimator (Theil, 1950; Sen, 1968) which is robust to outliers. The significance of trend signals was tested with the Mann-Kendall test (Mann, 1945; Kendall, 1948). Because various time series analyzed in the present study are serially correlated, pre-whitening (i.e., accounting for lag-1 autocorrelation) was incorporated in the test (Wang and Swail, 2001; Zhang and Zwiers, 2004) in order to avoid over-detection of trend significance (Bayazit and Önöz, 2007). For the count data of the climate change indices TX90p, TN10p, and WDcount, trends were estimated by logistic regression (Frei and Schär, 2001). Possible overdispersion due to fluctuating probabilities and serial correlation was taken into account (Frei and Schär, 2001). All trend signals were regarded as significant in case of a p -value ≤ 0.05 . If a time series did not cover the entire time period between 1981 and 2018, the fitted trend line was extrapolated.

To make atmospheric changes spatially comparable, absolute trends were converted to relative trend signals, except for parameters for which relative trends are not meaningful (i.e.,

³http://etccdi.pacificclimate.org/list_27_indices.shtml

TABLE 1 | Climate change indices analyzed in the present study.

ID	Index name	Index definition	Unit
DTR	Diurnal temperature range	Difference between daily maximum and minimum temperature	°C
TX90p	Warm days	Count of days when the daily maximum temperature centered on a 5-day window > 90th percentile	days
TN10p	Cool nights	Count of days when the daily minimum temperature centered on a 5-day window < 10th percentile	days
SDII	Simple precipitation intensity index	PRCP sum on wet days (PRCP ≥ 1 mm) divided by the count of wet days	mm day ⁻¹
WDcount	Wet day count	Count of days with PRCP ≥ 1 mm	days
CDD	Maximum length of dry spell	Maximum number of consecutive days with PRCP < 1 mm	days

The indices are identical to the ETCCDI climate change core indices (DTR, SDII, CDD), slightly adapted (TX90p, TN10p), and additional (WDcount).

temperature, DTR, TX90p, TN10p). In case of the climatic water balance, trend signals were normalized by dividing them by the standard deviation of the detrended time series in order to increase spatial comparability.

The impact of elevation on climate trend signals was estimated with linear regression. Correlation between atmospheric parameters were quantified with the Pearson's product-moment correlation coefficient.

Identification of Atmospheric Impacts on Scots Pine Vitality

The impacts of anomalies of atmospheric parameters and indices on defoliation change were identified and quantified with simple and multiple linear regression models. A large number of atmospheric variables and indices on different time scales and in different combinations were tested as explanatory variables. Because of the limited amount of suitable observational data, the models were kept relatively simple in order to reduce the risk of randomly inflating the explanatory power. Furthermore, we corroborated the findings of the regression analyses by the evidence of additional data sources and analyses. To avoid biased conclusions due to overfitting, the models were evaluated by comparing their Bayesian information criteria (BIC). For a more comprehensive model evaluation, we additionally included the Akaike information criteria (AIC), which penalize a higher number of explanatory variables less heavily. The explanatory power was quantified by the adjusted R^2 , which also accounts for the number of explanatory variables. Mortality time series were not used for regression analyses because defoliation change was found to react more directly and immediately to atmospheric stressors. Instead, we investigated the relationship between defoliation change and mortality as the ultimate and most obvious state of non-vitality.

RESULTS

Temporal Development of Scots Pine Vitality and Mortality

The magnitude and temporal development of Scots pine defoliation changes and mortality rates in the Swiss Rhône valley strongly varied spatially (Figure 2). Of the four forest plots analyzed, pronounced defoliation and mortality events only occurred near Visp, namely around 1999, 2004, 2011,

and 2017. The rare recovery of mean crown foliation (negative values in Figure 2) of surviving trees (e.g., 2001 and 2006) could by far not compensate the defoliation increase in other years. Hence, the capacity of Scots pines to recover has been generally low and seems even to have decreased over time (hardly any mean defoliation reduction since 2009). As a result, the average defoliation increased between 1996 and 2018 by 5.7% per year with an average annual mortality rate of 7.0%. The number of living Scots pines on the forest plot near Visp decreased by 72% from 78 to 22 within 22 years. The Pearson product moment correlation coefficient between defoliation change and mortality rate was 0.73 (p -value < 0.005). The mortality of individual trees occurred abruptly, as they had a median defoliation of only 25% until the median defoliation increased to 40% in the year before the reported tree death.

At the forest plot in Pfywald, the defoliation increased annually by 1.5% between 2003 and 2018 with a mean mortality rate of 1.7%, resulting in a total decrease of living Scots pines by 13% from 290 to 251 within 15 years. Compared to Visp, the decline occurred much more evenly distributed in time. Because of the low variability of defoliation change and mortality rate, the two parameters were not significantly correlated ($r = 0.44$, p -value = 0.10). In contrast to the forest plot near Visp, the defoliation of individual trees that died was clearly elevated (median of 60%) on a longer term before increasing to 65% 3 years and to 75% in the last year before mortality.

The forest plots at higher altitudes near Saillon and Lens were dominated by short-term oscillations between defoliation increase and decrease. This pattern and the relatively high magnitudes of annual defoliation change and occasional mortality may be partly explainable by the low number of annually monitored Scots pines on these two forest plots. Still, there are no clear indications for pronounced defoliation and mortality events. Because of the rare mortality of single trees, correlations between defoliation change and mortality rate were low and not significant.

Climatic Changes in the Region of the Rhône Valley

Reference Evapotranspiration and Vapor Pressure Deficit

On the annual time scale, the ETo increased at all weather stations except one (Figure 3A) with a median of +7.3% in the 38-year period from 1981 to 2018. However, there are strong

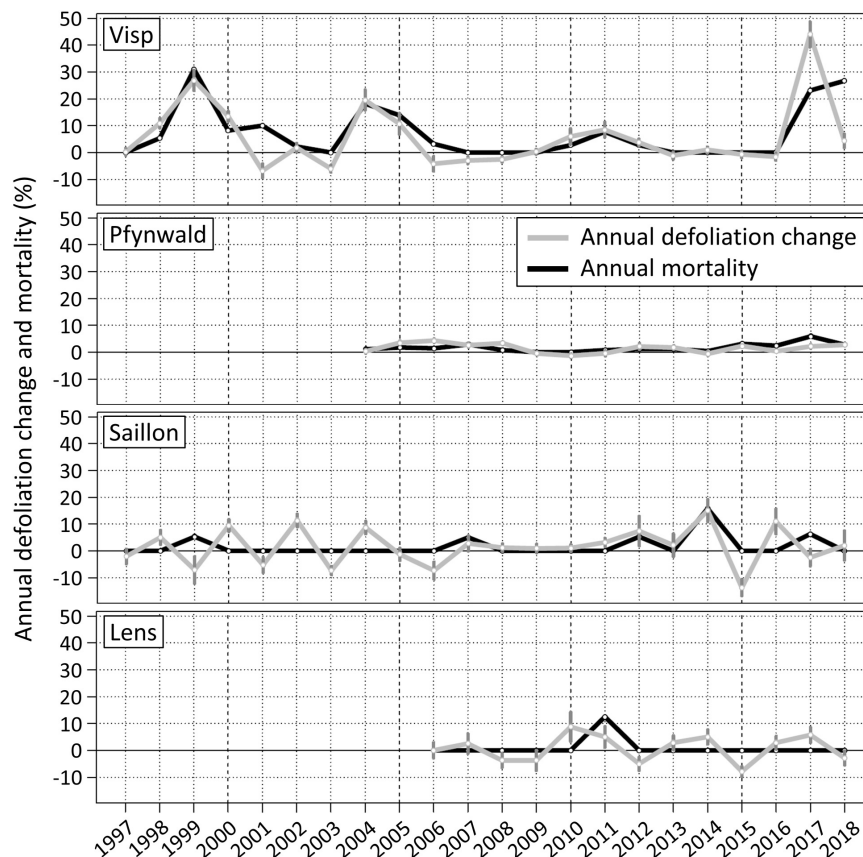


FIGURE 2 | Annual mean defoliation changes and mortality rates at the forest plots near Visp (mean $n = 47$), Pfywald (mean $n = 270$), Saillon (mean $n = 18$) and Lens (mean $n = 8$). The dark gray vertical bars represent the standard error of the mean of the annual defoliation change (average Visp = 2.1%, Pfywald = 0.4%, Saillon = 3.0%, Lens = 3.1%).

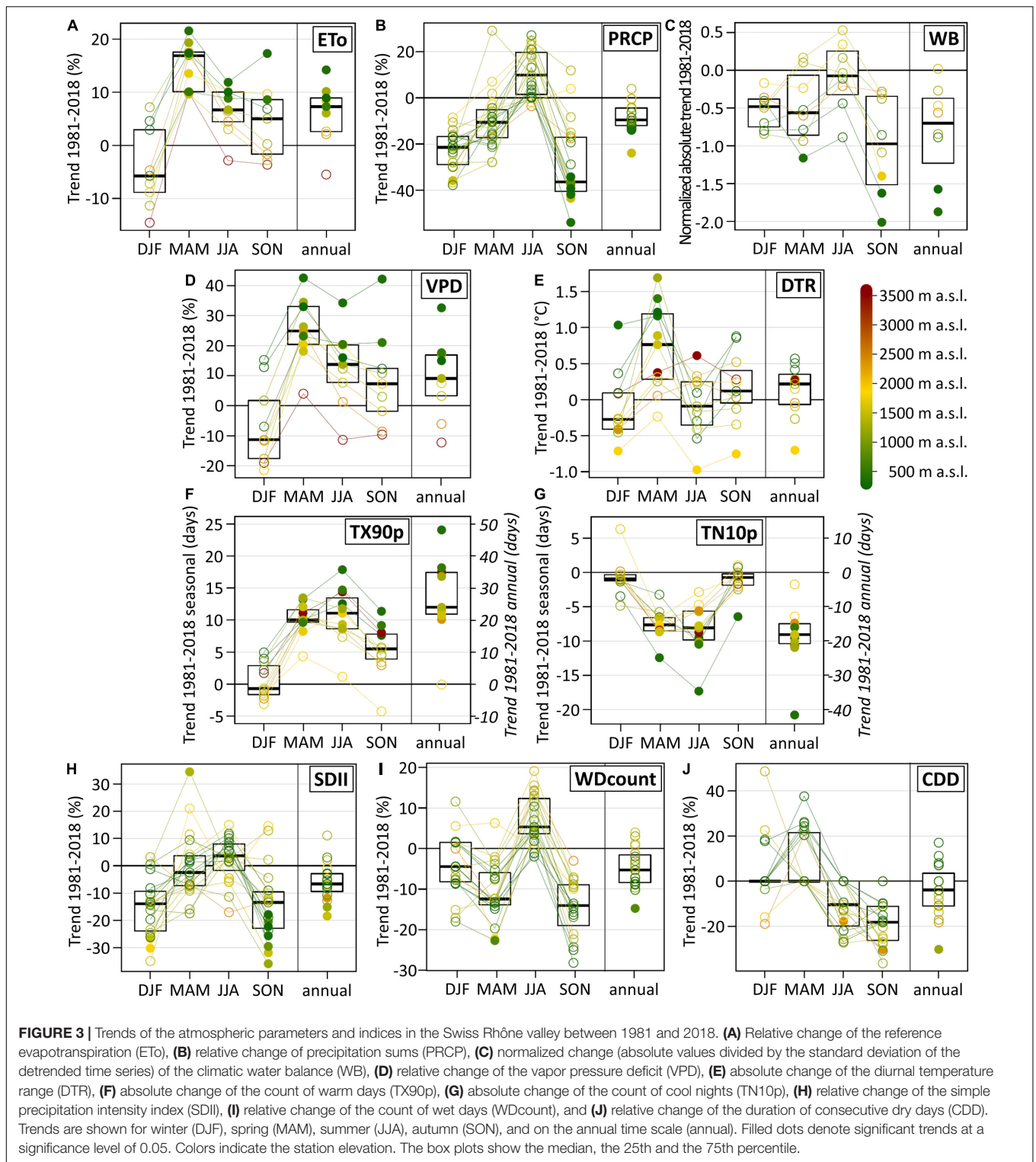
seasonal differences. Whereas percentual ETo trend signals in winter were insignificant with a high spread between the single stations, there was a pronounced significant increase in spring at all stations with a median of +16.9%. Seasonal trend patterns of the VPD were similar to those of the ETo, but VPD trend magnitudes and the spread of individual station trends were larger (Figure 3D). Same as for the ETo, the strongest VPD increase occurred in spring with a median of +24.9%.

On most time scales, percentual ETo trends were elevation dependent (Figure 3A and Supplementary Figure 1). This effect was particularly pronounced on the annual time scale (regression coefficient between elevation and the ETo = 0.76, p -value < 0.005) and in summer ($R^2 = 0.75$, p -value < 0.005). Below 1,500 m a.s.l., the ETo increased significantly at all individual stations on the annual time scale, in summer and in spring (with one exception). A similar but even stronger elevation dependence was found for VPD trend signals (Figure 3D and Supplementary Figure 1).

ETo trend signals of each meteorological station are based on the changes of the single atmospheric variables (Supplementary Figure 2) and their spatio-temporal impact and combination. The main driver of the increasing ETo in the Swiss Rhône

valley was air temperature (Supplementary Figure 3). The 1981–2018 temperature trends caused significant ETo increases at all investigated weather stations in spring, summer and on the annual time scale. Temporal changes of relative humidity, in contrast, mostly resulted in positive and significant ETo trends below 1,000 m a.s.l. and in negative ETo trends above 2,000 m a.s.l. Therefore, relative humidity induced a pronounced elevation dependence of ETo trend signals, particularly in summer ($R^2 = 0.86$, p -value < 0.005) and on the annual time scale ($R^2 = 0.91$, p -value < 0.005). Changes of the sunshine duration mostly caused positive ETo trends in spring, summer, and on the annual time scale. Temporal wind speed changes affected ETo trends only locally. The strongest impact occurred in Visp, where decreasing wind speed caused negative ETo trends, and hence lowering the overall ETo increase driven by the other variables.

For annual and seasonal ETo variability and extremes, temperature and relative humidity have the strongest overall impact (Supplementary Figure 4). Each of the two atmospheric variables explains between 20 and 40% of the total ETo variability at most station sites. Sunshine duration explains also 20–40% in spring and summer. Variability of wind speed is of minor importance but may locally still explain up to about 20% of the seasonal ETo variability.



Precipitation and Climatic Water Balance

PRCP sum time series are highly variable in time, and individual station trends are mostly insignificant except in autumn (**Figure 3B**). On the annual time scale, there are negative PRCP trends at all stations (except one) with a median of -9.6%.

PRCP sums decreased at most stations in winter, spring, and autumn, whereas they increased in summer. The seasonal PRCP trend cycle seems independent of the seasonal ETo trend cycle (**Figures 3A,B**). Hence, a PRCP decrease does not imply an ETo increase nor vice versa.

The climatic water balance as integrating factor of water in- and output generally decreased (**Figure 3C**). The strongest trend magnitudes occurred at low elevation sites and in autumn, but individual station trends were mostly insignificant and spread strongly. In summer, the generally increasing ETo and PRCP trends partly canceled each other out in the climatic water balance trend signal.

Climate Change Indices

Trend signals of the diurnal temperature range (DTR) spread strongly between the different meteorological stations (**Figure 3E**). However, a pronounced and mostly significant DTR increase occurred in spring at lower elevations, indicating a shift towards drier conditions (i.e., less cloudy conditions and less water vapor in the air). The frequency of exceptionally warm days (TX90p) increased mostly significantly in all seasons except for winter (**Figure 3F**). The strongest seasonal increase occurred in spring and summer. Trend magnitudes of the frequency of exceptionally cool nights (TN10p, **Figure 3G**) are lower and mostly inverse to those of the frequency of warm days.

The pronounced temporal and spatial variability of PRCP manifests in the PRCP-based climate change indices by mostly insignificant and strongly spreading individual station trends. On the annual time scale, the PRCP intensity (SDII) decreased at most stations (**Figure 3H**). This decrease occurred largely in winter and autumn. The frequency of wet days (WDcount) also decreased on the annual time scale, with generally negative trends in spring and autumn but positive trends in summer (**Figure 3I**). The duration of consecutive dry days (CDD) mostly increased in spring, particularly at elevations below 1,000 m a.s.l. (**Figure 3J**). In summer and autumn, in contrast, this duration generally decreased.

Impacts of Climatic Changes on Soil Water Availability

Because Scots pine decline occurred on the low elevation forest plots in the Swiss Rhône valley, the seasonal cycle and temporal changes of soil water availability near Visp and in Pfywald were investigated. Data of the weather station in Visp are representative for the forest plot near Visp, whereas Pfywald is located 20 km west of Visp, about halfway between the meteorological stations in Visp and Sion (**Figure 1**, see station abbreviations VIS and SIO). Climate characteristics and trends in Pfywald were therefore assumed to be in between the observations from the two sites.

The general climate characteristics at lower altitudes are similar within the central Rhône valley, which is also reflected in the seasonal cycles of potential water in- and output in Visp and Sion (**Figure 4** and **Supplementary Table 2**). At both sites, the ETo clearly exceeds PRCP sums in spring and summer. PRCP sum time series are characterized by a strong year-to-year variability, which clearly exceeds the mostly insignificant 1981–2018 trend signals (**Supplementary Table 2**). In contrast, the inter-annual variability of the ETo is rather small, but the ETo increased strongly and significantly in time (in spring, summer, and on the annual time scale). As a

consequence of the trend-dominated characteristics of the ETo and the variability-dominated characteristics of PRCP, annual and seasonal anomalies of the climatic water balance follow closely the variability of PRCP sums. In Visp, for example, the regression coefficient between PRCP sums and the climatic water balance is 0.92 (p -value < 0.005) on the annual time scale with the strongest relationship in winter ($R^2 = 0.98$, p -value < 0.005) and the weakest relationship in summer ($R^2 = 0.86$, p -value < 0.005). Correlations between PRCP sums and the ETo are low and insignificant except for spring ($r = -0.53$, p -value < 0.005).

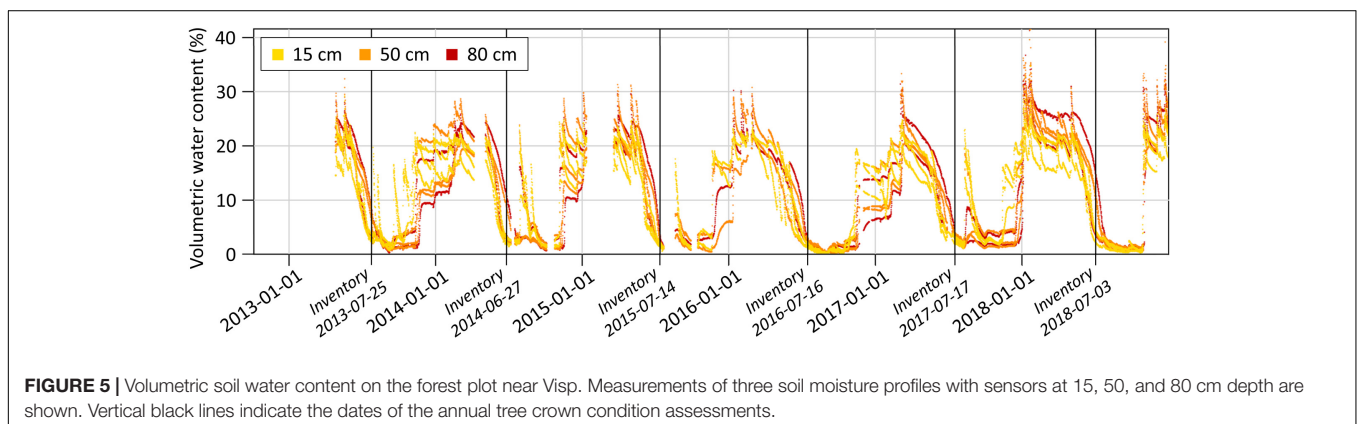
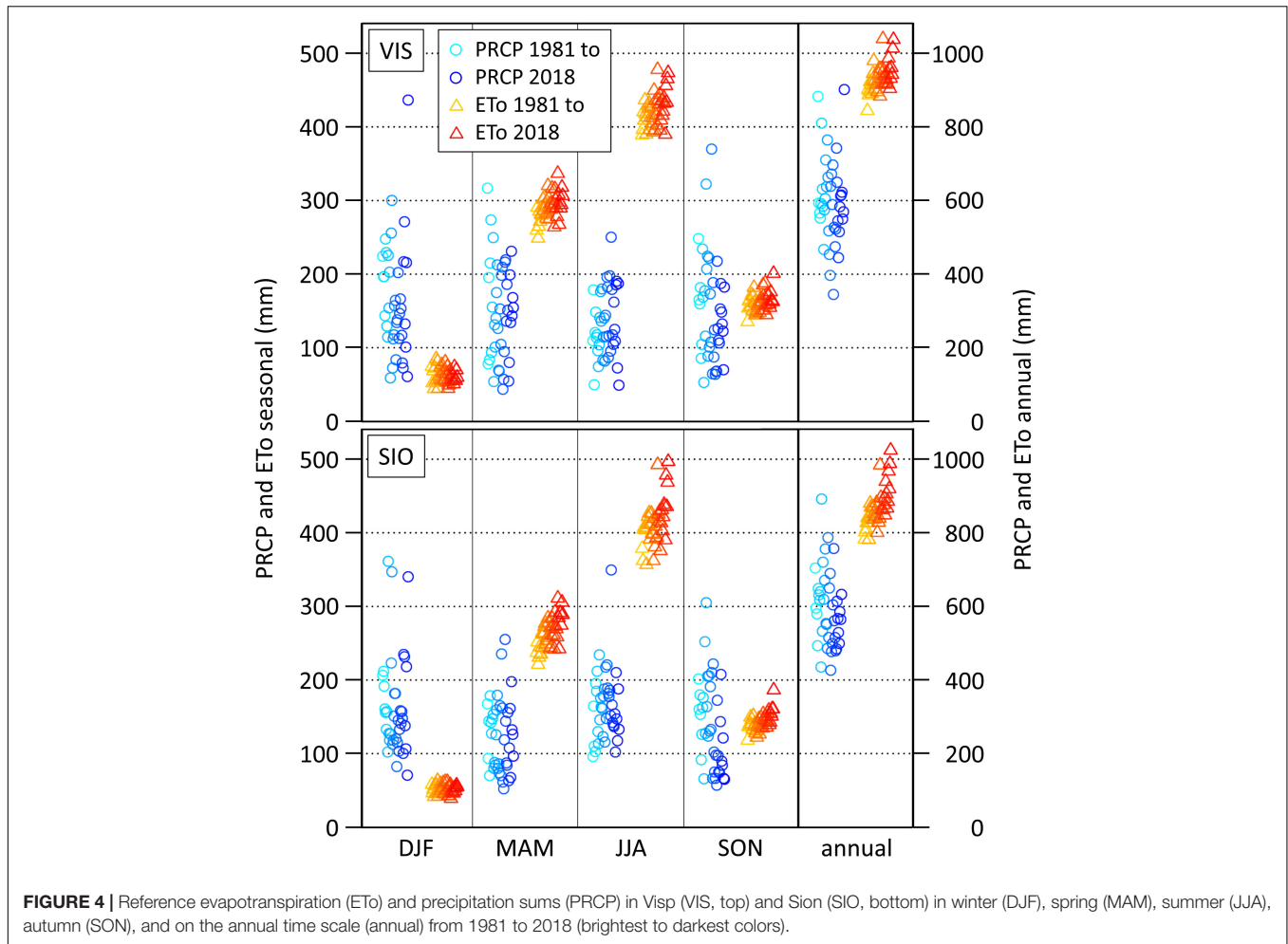
The strong excess of potential water output over water input in spring and summer in the central Rhône valley leads to yearly recurring periods of low soil moisture between midsummer and autumn. From 2013 to 2018 on the forest plot near Visp, for example, the volumetric soil water content fell regularly to low values around July (**Figure 5**). This drop occurred mainly independently of soil moisture contents in winter and spring. Substantial PRCP events between midsummer and autumn resulted in sudden soil moisture increases and prevented therefore prolonged and continuous periods of very low volumetric soil water contents in 2013, 2014, 2015, and 2017, but not in 2016 and 2018. Note that the annual tree health inventories usually took place shortly before very low soil moisture contents were reached.

Main Driver of Defoliation and Mortality Events

Negative July to September Precipitation Anomalies

Negative anomalies of PRCP patterns from midsummer to early autumn were the main driver of defoliation events on the forest plot near Visp from 1996 to 2018. Because crown defoliation assessments were mostly carried out in July, the effect of such PRCP anomalies did not manifest in the data of the same but the following year. We identified July to September as the most relevant period with wet day frequency (WDcount) and PRCP intensity (SDII) explaining about 60% of the defoliation change occurring until the next defoliation assessment (**Table 2**). This model has the lowest BIC and AIC values (indicating a higher quality than the other models) as well as the highest adjusted R^2 (highest explanatory power). Also, on longer time periods (estimated vegetation period from April to September, entire year) or if shifted by a month (JJA), the performance of this model is the best or among the best.

July to September PRCP sums explain about 50% of the defoliation change observed in the next year (**Table 2**). Hence, considering the temporal distribution of PRCP events (i.e., using WDcount and SDII instead of PRCP sums) may increase the explanatory power. There is an inverse relationship between July to September PRCP anomalies and the following annual defoliation change of Scots pines (**Figure 6**). Particularly, all four defoliation events followed clearly negative July to September PRCP sum anomalies. Only the clearly below average July to September PRCP sums in 1996 and 2006 did not trigger defoliation increases in the following years 1997 and 2007,



respectively, which can be explained by an above average wet day frequency and an evenly distributed temporal wet day occurrence.

Except for the period July to September, the explanatory power of the climatic water balance (WB) is slightly lower than the one of PRCP sums (Table 2). As demonstrated earlier, temporal anomalies of the climatic water balance closely follow PRCP sums. In July to September from 1996

to 2017, the regression coefficient between PRCP sums and the climatic water balance was 0.89 (p -value < 0.005) and the correlation coefficient between PRCP sums and the ETo -0.55 (p -value < 0.005). Adding the ETo as additional explanatory variable to PRCP sums or to WDcount and SDII results in a decrease of the model quality. Hence, year-to-year ETo anomalies did not or only marginally impact the defoliation of Scots pines in Visp.

TABLE 2 | Most relevant explanatory variables for defoliation changes on the forest plot near Visp in various time periods.

	Explanatory variables	July to September (previous year)	April to September (previous year)	Complete previous year	MAM (previous year)	JJA (previous year)	SON (previous year)	April to June (current year)
Multiple linear regression	WDcount + SDII	Adj. R^2 : 0.59 BIC: 161 AIC: 156	Adj. R^2 : 0.22 BIC: 174 AIC: 170	Adj. R^2 : 0.26 BIC: 173 AIC: 169	Adj. R^2 : 0.05 BIC: 179 AIC: 175	Adj. R^2 : 0.46 BIC: 166 AIC: 162	Adj. R^2 : -0.03 BIC: 181 AIC: 176	Adj. R^2 : -0.01 BIC: 180 AIC: 176
	WDcount + SDII + ETo	Adj. R^2 : 0.56 BIC: 164 AIC: 158	Adj. R^2 : 0.18 BIC: 177 AIC: 172	Adj. R^2 : 0.22 BIC: 176 AIC: 171	Adj. R^2 : 0.00 BIC: 182 AIC: 177	Adj. R^2 : 0.44 BIC: 169 AIC: 163	Adj. R^2 : -0.08 BIC: 184 AIC: 178	Adj. R^2 : -0.06 BIC: 183 AIC: 178
	PRCP sum + ETo	Adj. R^2 : 0.49 BIC: 165 AIC: 161	Adj. R^2 : 0.20 BIC: 175 AIC: 171	Adj. R^2 : 0.17 BIC: 176 AIC: 172	Adj. R^2 : 0.03 BIC: 179 AIC: 175	Adj. R^2 : 0.27 BIC: 173 AIC: 169	Adj. R^2 : -0.06 BIC: 181 AIC: 177	Adj. R^2 : 0.00 BIC: 180 AIC: 176
Simple linear regression	PRCP sum	Adj. R^2 : 0.50 (-) BIC: 163 AIC: 160	Adj. R^2 : 0.24 (-) BIC: 172 AIC: 169	Adj. R^2 : 0.21 (-) BIC: 173 AIC: 170	Adj. R^2 : 0.12 BIC: 176 AIC: 173	Adj. R^2 : 0.30 (-) BIC: 170 AIC: 167	Adj. R^2 : -0.01 BIC: 178 AIC: 175	Adj. R^2 : 0.04 BIC: 177 AIC: 174
	WB	Adj. R^2 : 0.51 (-) BIC: 163 AIC: 159	Adj. R^2 : 0.20 (-) BIC: 173 AIC: 170	Adj. R^2 : 0.19 (-) BIC: 173 AIC: 170	Adj. R^2 : 0.05 BIC: 177 AIC: 174	Adj. R^2 : 0.26 (-) BIC: 172 AIC: 168	Adj. R^2 : -0.01 BIC: 178 AIC: 175	Adj. R^2 : 0.03 BIC: 177 AIC: 174
	WDcount	Adj. R^2 : 0.24 (-) BIC: 172 AIC: 169	Adj. R^2 : 0.05 BIC: 177 AIC: 174	Adj. R^2 : -0.03 BIC: 179 AIC: 176	Adj. R^2 : -0.03 BIC: 179 AIC: 175	Adj. R^2 : 0.31 (-) BIC: 170 AIC: 167	Adj. R^2 : -0.05 BIC: 179 AIC: 176	Adj. R^2 : -0.05 BIC: 179 AIC: 176
	SDII	Adj. R^2 : 0.27 (-) BIC: 171 AIC: 168	Adj. R^2 : 0.16 (-) BIC: 174 AIC: 171	Adj. R^2 : 0.28 (-) BIC: 171 AIC: 167	Adj. R^2 : 0.01 BIC: 176 AIC: 173	Adj. R^2 : 0.15 (-) BIC: 174 AIC: 171	Adj. R^2 : 0.01 BIC: 178 AIC: 174	Adj. R^2 : 0.04 BIC: 177 AIC: 174
	ETo	Adj. R^2 : 0.23 (+) BIC: 172 AIC: 169	Adj. R^2 : 0.03 BIC: 177 AIC: 174	Adj. R^2 : 0.00 BIC: 178 AIC: 175	Adj. R^2 : -0.04 BIC: 179 AIC: 176	Adj. R^2 : 0.01 BIC: 178 AIC: 175	Adj. R^2 : -0.05 BIC: 179 AIC: 176	Adj. R^2 : -0.03 BIC: 179 AIC: 176

The best model [i.e., lowest Bayesian information criterion (BIC) and Akaike information criterion (AIC), highest adjusted R^2] is highlighted in green. Models with a BIC ≤ 164 are marked in dark gray, with a BIC ≤ 166 in gray, with a BIC ≤ 170 in light gray, and with a BIC ≤ 174 in very light gray. Adjusted R^2 of models with p -values ≤ 0.05 are highlighted in bold font. For the simple linear regression models, the signs of the relationship ("+" for positive and "-" for negative) are shown in brackets in case of significance. The explanatory variables in the table include the count of wet days (WDcount), simple precipitation intensity index (SDII), reference evapotranspiration (ETo), precipitation sum (PRCP sum) and climatic water balance (WB). April to September is the estimated vegetation period. MAM abbreviates the spring months, JJA the summer months, and SON the autumn months. April to June of the current year is the vegetation period directly before the crown defoliation assessment. Note that many further explanatory variables, variable combinations and time periods were tested, but the quality of these models was low (BIC > 172, AIC > 169, and adjusted R^2 < 0.20).

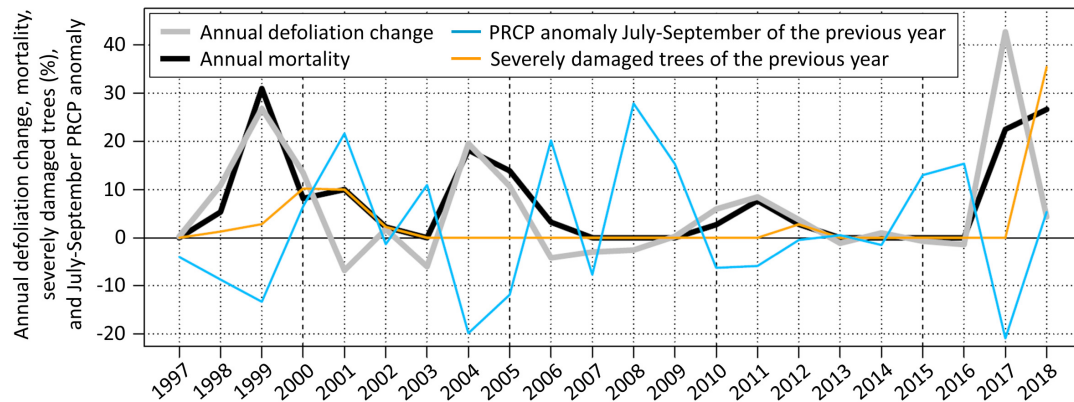


FIGURE 6 | Annual defoliation change, mortality rates, precipitation sum (PRCP) anomalies from July to September of the previous year, and the fraction of severely damaged living trees ($\geq 75\%$ defoliation) of the previous year on the forest plot near Visp. PRCP anomalies were normalized by dividing by the detrended standard deviation of the time series and subtracting the 1996–2017 mean. The anomalies were multiplied by 15 in order to match the scale of the annual defoliation change. Anomalies of PRCP sums and not anomalies of PRCP frequency and intensity (higher explanatory power) are shown in order to facilitate the visual interpretation.

Atmospheric conditions in time periods before midsummer and after early autumn (i.e., spring and autumn of the previous year, vegetation period before the defoliation assessment) have no or only marginal impact on the defoliation variability of Scots pines (Table 2). In the present study, the impact of longer-term periods on defoliation change may be actually overestimated, because the correlation of PRCP sums of the entire year and from July to September was exceptionally high between 1996 and 2017 ($r = 0.73$, p -value < 0.005) compared to 1981–2018 ($r = 0.31$, p -value = 0.06). Furthermore, annual PRCP anomalies on the annual time scale and during the vegetation period strongly deviated from July to September PRCP anomalies in single years (Supplementary Figure 5). The extreme defoliation event in 2017, for instance, followed extremely low July to September PRCP sums in 2016, but annual PRCP sums in 2016 were on average and PRCP sums in the vegetation period in 2016 were only moderately low.

Same as in the Swiss Rhône valley, Scots pine dieback events in other European regions directly followed strongly negative July to September PRCP anomalies. This applies to other Alpine areas with mortality events in 1997 in the Inn valley in Austria (Cech and Perny, 2000), 2003 in the Adige valley in Italy (Minerbi et al., 2006), and 2005 in the Aosta valley in Italy (Gonthier et al., 2010), but also to regions beyond the Alps such as 2000 and 2012 in Romania (Sidor et al., 2019), 2005 in the central Pyrenees in Spain (Galiano et al., 2010), and 2015 in Franconia in Germany (Buras et al., 2018). In most of these cases, the July to September PRCP sum anomalies were more negative than those of the vegetation period (April to September) or the complete year, which indicates a critical impact of low midsummer to early autumn PRCP beyond the Swiss Rhône valley.

Local Climate Characteristics

Despite the similar water in- and output in the central Rhône valley (Figure 4), temporal defoliation patterns varied strongly within short distances such as on the forest plots near Visp and in Pfywald (Figure 2). A notable difference of local climate

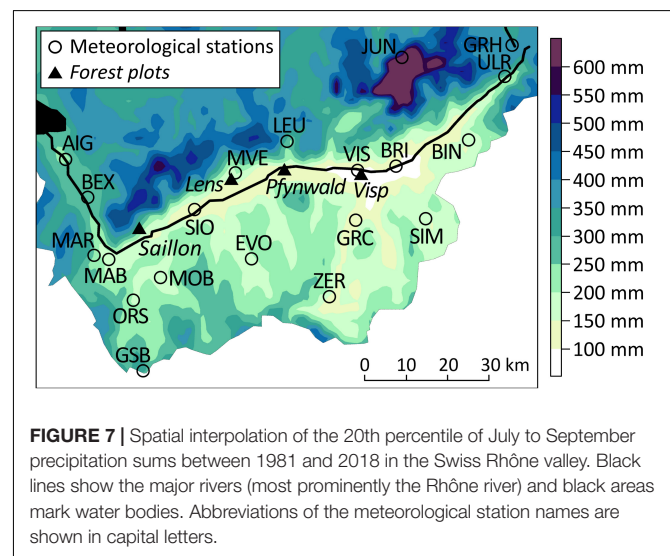


FIGURE 7 | Spatial interpolation of the 20th percentile of July to September precipitation sums between 1981 and 2018 in the Swiss Rhône valley. Black lines show the major rivers (most prominently the Rhône river) and black areas mark water bodies. Abbreviations of the meteorological station names are shown in capital letters.

characteristics between the two sites are the lower PRCP sum minima between midsummer and early autumn around Visp (Figure 7). The forest plot near Visp is centrally located in the area where July to September PRCP sums of events with a 5-year return period are lowest. July to September PRCP sums < 100 mm occurred several times in Visp (VIS), but not further west in Sion (SIO) (see also Figure 4). A 20th percentile of July to September PRCP sums < 100 mm might therefore roughly describe a critical threshold for the occurrence of regular Scots pine defoliation events in the Swiss Rhône valley since the 1990s.

Further Impact Factors on Defoliation and Mortality Events

Spring Frost

Around April 20 in 2017, a strong multi-day spring frost occurred in large parts of Europe at a point of time when

the number of accumulated growing degree days was already high (Vitasse and Rebetez, 2018; Zohner et al., 2020). This frost event was unprecedented in terms of the damage risk for vegetation since the start of instrumental weather observations in several regions in Switzerland (Vitasse and Rebetez, 2018). Its occurrence coincided with the time of the lowest frost hardness of Scots pine needles of about -8°C (Bachofen et al., 2016). At the meteorological station in Visp, temperatures fell as low as -5.5°C . However, in clear and windless nights such as around the frost event, temperatures of plant tissues may be $4-8^{\circ}\text{C}$ lower than temperatures measured at 2 m height under sheltered conditions because of radiative cooling (Ducrey, 1998). Hence, there was a high risk for frost damage on the forest plot near Visp. CIR imagery derived from satellite earth observations before and after the frost event indicates frost damages on Scots pines and other vegetation near Visp (example shown in **Supplementary Figure 6**). Furthermore, extensive frost damage on shoot increments of Scots pines was observed on a forest stand between 800 and 950 m a.s.l. about 20 km west of Visp (personal communication with Pierre Vollenweider).

The spring frost in 2017 may have substantially contributed to the exceptionally high 44% Scots pine defoliation change observed near Visp in July 2017 (**Figure 6**). From July to September 2016, PRCP intensity and frequency anomalies were strongly negative, and Scots pine dieback in the region of Visp was already reported in October 2016 (Rigling et al., 2018). The combination of water stress in 2016 and the spring frost 2017 seems to have strongly deteriorated the vitality of Scots pines.

Pests and Pathogens

On the forest plot near Visp, pests and pathogens intensified and prolonged particularly one Scots pine defoliation and mortality event. In 1999, 82% of the tree crowns were damaged by insects and 30% by fungi. Around Visp and in further areas in the Rhône valley, Scots pines were strongly infested by the pine shoot beetle (*Tomicus piniperda*) and the fungus *Cenangium ferruginosum* (information provided by Waldschutz Schweiz). These biotic factors increased the annual defoliation change in 1999 by more than 10% and explain therefore about a third of the total 27% defoliation change (**Figure 6**). In 2000, the insect and fungus infestation was still intense with 76 and 14% affected trees, respectively. Removing the impact of these biotic factors from the defoliation change time series results in a more proportional reflection of the magnitude of negative July to September PRCP sum anomalies compared to the other events.

The pest and pathogen infestation in 1999 and 2000 on the forest plot near Visp was clearly the most severe biotic damage impact between 1996 and 2018. In all other years, the percentage of Scots pines with reported insect damage remained below 20%, and the impact on defoliation change was therefore rather small. Before the infestation in 1999, Scots pines were exposed to four consecutive years with negative July to September PRCP sum anomalies (**Supplementary Figure 5**). This exceptionally long stress period may have favored the intense insect and fungi infestation.

Defoliation Exceedance Over a Point of No Return

In contrast to the defoliation change, tree mortality on the forest plot near Visp sometimes still occurred a few years after negative July to September PRCP sum anomalies. This prolonged mortality can be largely explained by the fraction of severely damaged trees (**Figure 6**). A high fraction of severely damaged trees results in pronounced prolonged mortality (after the 1999 and 2017 event), whereas mortality decreases quickly if only a small fraction of trees is severely damaged (after the 2004 and 2011 event). If accounting for the fraction of severely damaged trees (i.e., shifting the occurrence of mortality of the trees that died to the year when the defoliation threshold was exceeded), the correlation coefficient between defoliation change and mortality rate increases from 0.73 to 0.94 (p -value < 0.005 in both cases) (**Supplementary Figure 5**).

In this study, severely damaged trees were defined as trees that exceeded a defoliation threshold (point of no return) that leads most likely to mortality within 2 years. Scots pines exceeding such defoliation thresholds may not be able to maintain important physiological functions and die likely from carbon starvation (Galiano et al., 2011; Guada et al., 2016; Schönbeck et al., 2018). On the monitored forest plot near Visp, most Scots pines that reached a crown defoliation $\geq 75\%$ died within 1 (70%) or 2 years (83%) without being exposed to further water stress. This causes a pronounced bimodal distribution of the defoliation magnitude in the last year before mortality. The defoliation before mortality of most trees was low (median of 35% if including defoliation values $< 70\%$), whereas it was high for the trees that past the point of no return (median of 85% if including defoliation values $\geq 70\%$).

DISCUSSION

Atmospheric Pathways to Defoliation and Mortality Events

Despite the critical importance of July to September PRCP on the vitality of Scots pine from the 1990s onwards, the water input in summer mostly increased in the Swiss Rhône valley from 1981 to 2018 (**Figure 3**). In Visp, for example, summer PRCP sums increased by 23 mm. This trend cannot be explained by a single factor such as more extreme PRCP events, because the wet day frequency (WDcount) increased as well as the PRCP intensity (SDII), whereas the consecutive dry day duration (CDD) decreased. Hence, temporal changes of the water input patterns in summer are not responsible for the emergence of July to September PRCP anomalies as the main driver of sudden Scots pine vitality declines on the forest plot near Visp.

The most consistent change from 1981 to 2018 in the Swiss Rhône valley's climate regime occurred in spring with a pronounced shift toward drier conditions particularly at lower altitudes. The ETo and the VPD increased strongly, whereas PRCP related parameters and indices consistently indicate a decrease in spring water input (**Figure 3**). The atmospheric water demand also increased in summer. These changes consequentially prolonged and intensified the annual

period of low soil moisture. In Visp, this period usually started in July (**Figure 5**), coinciding with the beginning of the period during which substantial PRCP events are critical for the Scots pine vitality. Midsummer to autumn periods of continuously low soil water contents such as in 2016 seem to trigger sudden defoliation increases as observed in the monitoring campaign in July 2017 (**Figure 7**). In these cases, Scots pines most likely suffered from xylem cavitation, which represents a critical point in the drought response pathway (Choat et al., 2018; Grossiord et al., 2020) and results in increased crown defoliation (Rood et al., 2000) or even in rapid mortality (e.g., Bréda et al., 2006; McDowell et al., 2008; Brodribb and Cochard, 2009; Arend et al., 2021). Tree damage caused by soil drought is largely dictated by the reached extreme of negative water potential and the amount of time spent at this extreme (Choat et al., 2018). Major rain events within a dry period, however, may result in a fast re-initiation of soil water uptake (Gessler et al., 2022) and thus recovery of important physiological tree functions (Skelton et al., 2017).

On the forest plot near Visp, already moderately below average July to September PRCP sums triggered pronounced defoliation and mortality events. Hence, such events may occur even in absence of rare atmospheric extremes, because trend-dominated changes (i.e., the increase of atmospheric water demand in spring and summer) may alter critical thresholds for variability dominated parameters (i.e., July to September PRCP). This illustrates the importance of analyzing water in- and output individually. Approaches combining them such as the climatic water balance may hide important temporal changes and variability differences. As trend signals of atmospheric parameters and indices strongly vary between the seasons as well as the tree's sensitivities to disturbances within the phenological cycle (Badeck et al., 2004; Holst et al., 2008; Anderegg et al., 2013; Bose et al., 2020), it is important to analyze atmospheric trends and anomalies on intra-annual time scales. Furthermore, spatial gradients of trend signals should be considered in analyses on water stress. This is illustrated by the elevation dependence of the temporal changes of the atmospheric water demand in the Swiss Rhône valley, which results in an increase of water stress particularly at low elevations where Scots pines are already at the dry edge of their distribution (Rigling et al., 2013; Schönbeck et al., 2018).

July to September Precipitation Minima Define Most Affected Region

Spatial climate characteristics corroborate the role of low midsummer to early autumn PRCP as driver of sudden Scots pine vitality declines. The area with the lowest 20th percentile of July to September PRCP sums coincides with the area in the Rhône valley that has been most affected by sudden defoliation and mortality events since the 1990s. The mortality event starting in October 2016, for instance, affected the region Brig-Visp-Stalden-Turtmann (Rigling et al., 2018), which is the region extending about 10–15 km to the west and east of Visp and ca. 10 km to the south. In contrast to the forest plot near Visp, the forest plot in Pfywald is located outside the area of

the lowest 20th percentile of July to September PRCP sums, and Scots pines were therefore less exposed to extreme and long-lasting negative soil water potentials and thus no clear mortality peaks occurred.

The differences in water stress levels and mortality trajectories of individual trees (sudden and strong defoliation increase near Visp and gradual increase in Pfywald) may suggest different dominant processes leading to tree mortality. While hydraulic failure is the likely cause of Scots pine mortality events near Visp, Schönbeck et al. (2018) showed that carbon starvation is related to Scots pine mortality in Pfywald. Considering that intense short-term water stress may lead to mortality by hydraulic failure, whereas intermediate longer-term water stress rather results in mortality by carbon starvation (McDowell et al., 2008; Gessler et al., 2018), one may speculate that these different pathways to mortality explain the occurrence of pronounced dieback events near Visp, whereas the mortality rate in Pfywald is rather constantly elevated and might affect trees that show low vitality since longer time periods. Since xylem cavitation and carbon starvation are often not independent processes (Anderegg and Callaway, 2012; Gessler et al., 2018), this may describe the dominant but not exclusive processes at the two sites.

Importance of Further Factors on Defoliation and Mortality Events

Except for the spring frost in 2017, no further atmospheric anomalies and extremes other than low July to September water input were identified as substantial drivers of defoliation and mortality events in the Swiss Rhône valley. Nevertheless, temporal changes which not exclusively affect soil water availability may have contributed to increase the tree stress. For instance, the VPD increased strongly from 1981 to 2018 at lower elevations (**Figure 3D**). An increasing VPD may lower growth rates even if sufficient soil water is available (Zweifel et al., 2016; Etzold et al., 2018; Grossiord et al., 2020). Furthermore, there was a strong increase of the frequency of hot days (**Figure 3F**) and the daily maximum temperatures (**Supplementary Figure 2A**). Extreme heat may affect various tree functions, decrease growth, and, in combination with water stress, lead to mortality (e.g., Park Williams et al., 2013; Teskey et al., 2015). Previous studies detected decreasing Scots pine growth at lower elevations in the central part of the Swiss Rhône valley (e.g., Timofeeva et al., 2017; Rigling et al., 2018; Bose et al., 2020), and low tree growth can increase the risk for tree mortality (Bigler et al., 2006; Guada et al., 2016).

The predisposition of Scots pines to water stress events also depends on previous conditions the trees have been exposed to (e.g., Bose et al., 2020; Zweifel et al., 2020). Scots pines affected by drought stress can build a more effective water-conducting system by increasing lumen width and decreasing cell-wall thickness at the cost of a higher vulnerability to cavitation and reduced growth (Eilmann et al., 2011; Martin-Benito et al., 2013, 2017). Because of several phases of particularly high water stress in the region around Visp within recent decades, trees in this area may have

become more vulnerable to events of low midsummer to early autumn water input than Scots pines in other regions (including Pfywald).

Mistletoe infestation may be considered as predisposing and contributing factor by reducing the carbon assimilation capacity of trees and increasing their water loss to the atmosphere (Dobbertin and Rigling, 2006; Zweifel et al., 2012). The fraction of medium and strongly infested Scots Pines was related to the magnitude of crown defoliation and was highest for defoliations $\geq 60\%$. 33% of the Scots pines near Visp and 54% in Pfywald were moderately or strongly infested 1 year before their reported mortality. In accordance with Dobbertin and Rigling (2006), mortality rates of infested trees were disproportionately high within the single defoliation classes on the forest plot near Visp. This, however, was not the case for Pfywald, where mistletoes were much more prevalent. The percentage of infested trees decreased within the analyzed time period from 15% (first 5 years) to 5% (last 5 years) on the forest plot near Visp, and from 55% (first 5 years) to 37% (last 5 years) in Pfywald. Hence, the impact of mistletoe infestation was rather limited overall and may not explain the observed spatio-temporal vitality decline patterns in the Swiss Rhône valley.

Competition is a further predisposing factor (Rigling et al., 2013; Archambeau et al., 2020). The average density of living Scots pines and basal area on the forest plot near Visp were clearly lower than on the other analyzed forest plots, which was partly caused by the pronounced Scots pine decline. The competitive pressure was therefore higher on the other forest plots and it further decreased near Visp, of which the remaining Scots pines may have benefited (Giuggiola et al., 2013; Etzold et al., 2014; Madrigal-González et al., 2017). Note, however, that the number of shrubs increased after Scots pine dieback events, and the forest plot near Visp is therefore currently clearly more overgrown than the other forest plots. Nevertheless, our results do not indicate a substantial impact of competition on the occurrence of mortality and defoliation events.

In line with previous findings (e.g., Rebetez and Dobbertin, 2004; Dobbertin et al., 2007; Rigling et al., 2018; Jaime et al., 2019; MacAllister et al., 2019), our results indicate that pests and pathogens may intensify Scots pine defoliation and mortality events as a secondary driver by affecting already stressed and vulnerable trees. Particularly after multiple consecutive years of midsummer to early autumn periods of water stress, Scots pine forests seem to be susceptible to pest and pathogen outbreaks. However, during three of the four events of sudden vitality decrease on the forest plot near Visp, only minor biotic damages were observed. Biotic stressors were therefore not a necessary factor for severe dieback events.

On the forest plot near Visp, negative anomalies of the July to September water input had a fast effect on Scots pine defoliation, whereas mortality increased less immediately. We identified the fraction of trees exceeding a defoliation threshold arising after water stress events as the main cause for prolonged mortality. Nearly all of these trees were unable to recover and died within 2 years. If accounting for the fraction of

severely damaged trees, defoliation change and mortality rate were highly correlated. Notably, the fraction of such severely damaged trees strongly varied between the different dieback events (**Figure 6**). It was lowest when water stress seemed to be the only relevant impact (events around 2004 and 2011) and highest when biotic and frost damage was involved too (events around 1999 and 2017). We assume that severe crown defoliation caused by xylem cavitation (the probability of which might be increased by drought induced fine root mortality) impairs vital tree functions leading to death within a few weeks or months, whereas direct damage of needle and twig tissue (e.g., by frost or pathogens) may result in a slower pathway to mortality.

Outlook on the Scots Pine Population in the Rhône Valley

Future changes of midsummer to early autumn PRCP patterns as the main driver of sudden Scots pine vitality decline are of utmost importance. Whereas water input in summer was generally slightly increasing from 1981 to 2018, climate projections in the region of the Swiss Rhône valley indicate a decrease of summer PRCP sums (ca. -5% until 2035 -5% to -15% until 2060 and -5% to -25% until 2085 compared to the reference period from 1981–2010) in combination with a decrease of the wet day frequency and an increase of the duration of consecutive dry days (CH2018, 2018). Furthermore, the ETo will continue to increase, mostly because of the projected temperature rise, which is highest in summer when the relative humidity is projected to decrease (CH2018, 2018). Hence, midsummer to early autumn water stress phases will most likely continue to prolong and intensify in the coming decades. The projected increase of the frequency and magnitude of maximum temperature extremes in summer (CH2018, 2018) may additionally contribute to the tree stress.

Severe spring frost that can substantially damage adult Scots pines such as in 2017 have been rare events in the Swiss Rhône valley. However, the risk of such events may be increasing. Due to climatic changes, the start of the phenological growth period shifted to earlier in spring when the occurrence of severe frost is still more likely (Kellomaki et al., 1995; Vitasse and Rebetez, 2018; Vitasse et al., 2018; Zohner et al., 2020). Also the risk of pest and pathogen outbreaks may increase in future, because winter and spring temperatures, which are critical for the control of pests and pathogens (Rebetez and Dobbertin, 2004; Dukes et al., 2009), are projected to rise in coming decades in the Swiss Rhône valley (CH2018, 2018). At the same time, Scots pines will likely be more often affected from water stress and hence be more predisposed to such secondary disturbances.

A long-term dominance of a major Scots pine population at low elevations in the central Rhône valley seems unlikely considering the deterioration of tree vitality since the 1990s, the main drivers of these changes and the relevant climate projections. The occurrence of pronounced defoliation and mortality events will most likely extend to larger areas. Particularly the region west (i.e., down the valley) of Visp beyond Sion may become susceptible to such events, because it includes

large areas at low elevations including Pfywald, the general climate conditions are similar to those around Visp (**Figure 4**), July to September PRCP minima are relatively low (**Figure 7**), and trend magnitudes towards drier climatic conditions from 1981 to 2018 were exceptionally strong (**Supplementary Table 2**). Emerging defoliation and mortality events will accelerate the Scots pine decline and the already observed vegetation shift toward more drought-tolerant tree species such as pubescent oak (Weber et al., 2007; Rigling et al., 2013). However, regions at higher altitudes in the Rhône valley may remain suitable Scots pine habitats on longer time scales, because relative trend signals toward drier climate conditions decrease with increasing altitude and water stress mostly affects trees at lower elevations (Babst et al., 2013; Bose et al., 2020; Trotsiuk et al., 2020). Therefore, a soon extension of pronounced Scots pine defoliation and mortality events to higher altitudes seems unlikely.

Implications and Limitations

The main challenge to statistically identify atmospheric drivers of sudden Scots pine vitality decline is the scarceness of adequate observational data. Besides systematic long-term observations of crown defoliation and further relevant parameters on the annual time scale, Scots pines must be common on the monitored forest plots and should have been affected by ideally several sudden defoliation events. The comparability of time series from different forest plots and monitoring programs must be guaranteed. Furthermore, comprehensive long-term and high-quality meteorological data representative for investigated forest plots are required and the temporal homogeneity must be ensured if trends are analyzed as well. These requirements applied to the forest plots analyzed in the present study, but sudden defoliation and mortality events only occurred on the forest plot near Visp. Therefore, several analyses were based on observations at this site only, which increases the risk of biased conclusions. However, the defoliation and mortality events were not limited to this specific forest plot, but they affected larger areas around Visp (e.g., Rigling et al., 2018). Furthermore, various additional data sources and analyses corroborate the findings and provide a consistent and conclusive picture of the relevant drivers and processes responsible for the defoliation and mortality events in the Swiss Rhône valley. We also assume that the careful selection and preparation of adequate data and methods (e.g., using defoliation change instead of the mean defoliation) contributed to the consistency of the results.

Conditions on the different forest plots analyzed in the present study were overall similar regarding stem diameter, social position of trees, soil properties, etc. Some of the most notable differences between the forest plot near Visp and the other sites (basal area, mistletoe infestation) would rather indicate a lower predisposition to drought stress in Visp. Furthermore, such site-specific differences may affect the longer-term predisposition of the Scots pines, but not the year-to-year variability of tree vitality. Since the region with the lowest July to September PRCP sum minima outlines the area where most dieback events occurred (**Figure 7**), spatial differences in atmospheric water input seem to be more decisive for Scots pine vitality changes than other site-specific differences.

The findings of the present study are relevant beyond the region of the Swiss Rhône valley. First analyses indicated that strongly negative July to September PRCP anomalies are drivers of Scots pine dieback events in several further European regions, which suggests similar pathways to sudden mortality as in the Swiss Rhône valley. More detailed analyses that include local *in-situ* PRCP observations instead of rather coarsely gridded interpolations may further clarify the relevance of midsummer to early autumn PRCP patterns in these events.

The combination of comprehensive analyses of Scots pine vitality trajectories, climatic trends, local climate characteristics, and further relevant data provided new and more conclusive insights expanding the findings of previous research (e.g., Rebetez and Dobbertin, 2004; Eilmann et al., 2011; Rigling et al., 2013, 2018). Future research may test the findings of the present study on a continental level, for instance by analyzing suitable compiled Scots pine defoliation time series from forest sites all over Europe. This may allow more sophisticated model development (e.g., non-linear models) which may increase the explanatory power and model performance. Research projects on drought-related Scots pine mortality may focus more on the midsummer to early autumn period. Since the trends and anomalies of atmospheric parameters and indices affect the entire vegetation, the results of this study might be transferable to cases of recent vitality decline events of other tree species.

CONCLUSION

The atmospheric drivers causing the observed spatio-temporal Scots pine defoliation and dieback patterns are poorly understood. The present study addresses this issue by comprehensively analyzing data from long-term forest monitoring and climate observation in the Swiss Rhône valley. At lower elevations, there was a strong increase of the atmospheric water demand in spring and summer in the past decades which clearly exceeded its year-to-year variability. This constantly increased the risk of soil drought occurrence between midsummer and autumn. Scots pines became therefore critically dependent on substantial precipitation events, making below average precipitation frequency and intensity between July and September the main driver of sudden vitality declines and dieback events. Precipitation patterns during these months are dominated by a high year-to-year variability, whereas temporal changes are insignificant. Therefore, drought indices combining water in- and output such as the climatic water balance are less suitable to explain events of Scots pine vitality decline than precipitation patterns between midsummer and early autumn. To trigger such events, no rare atmospheric extremes are required because already moderately below average July to September precipitation may strongly affect tree vitality. Consequently, the area with the lowest precipitation minima define the region most affected by Scots pine dieback. Other impacts such as biotic stressors may intensify defoliation and mortality events, but they are not necessary factors. In the Swiss Rhône valley, the occurrence of dieback events will likely expand to larger areas

and accelerate the Scots pine decline. The main findings of the present study seem to be transferable to other European regions. The case of the Rhône valley provides exceptionally conclusive and consistent insights on drivers of Scots pine dieback, which may, beside others, increase the performance of vitality and mortality modeling. We therefore suggest to pay special attention to midsummer to early autumn water input patterns in related future studies and experiments.

DATA AVAILABILITY STATEMENT

Publicly available datasets were analyzed in this study. This data can be found here: <https://www.wsl.ch/en/forest/forest-development-and-monitoring/long-term-forest-ecosystem-research-lwf/data/data-request.html>; <http://icp-forests.net/page/data-requests>; and <https://www.meteoswiss.admin.ch/home/services-and-publications/beratung-und-service/datenportal-fuer-lehre-und-forschung.html>.

AUTHOR CONTRIBUTIONS

SH and AG conceptualized the study. MB and SS provided quality controlled and homogenized atmospheric data from the study region. SH collected and quality controlled the other data, performed the analyses, and led the writing of the manuscript. All

authors contributed to the writing and revision of the manuscript and approved the submitted version.

FUNDING

We acknowledge financial support by the Swiss National Science Foundation SNF (310030_189109) and we wish to thank the forest service of the Canton Valais for technical and financial support in the frame of the project: Déperissement du pin dans le Haut-Valais: Analyse des facteurs de mortalité. Open access funding provided by WSL—Swiss Federal Institute for Forest, Snow and Landscape Research.

ACKNOWLEDGMENTS

We thank Francesco Isotta (MeteoSwiss), Peter Waldner, Christian Ginzler, Sophie Stroheker, Christian Hug, Flurin Sutter, Beat Wermelinger, and the LWF field experts (all WSL) for the expert discussions and support.

SUPPLEMENTARY MATERIAL

The Supplementary Material for this article can be found online at: <https://www.frontiersin.org/articles/10.3389/ffgc.2022.874100/full#supplementary-material>

REFERENCES

- Allen, C. D., Breshears, D. D., and McDowell, N. G. (2015). On underestimation of global vulnerability to tree mortality and forest die-off from hotter drought in the Anthropocene. *Ecosphere* 6:art129. doi: 10.1890/ES15-00203.1
- Allen, C. D., Macalady, A. K., Chenchouni, H., Bachelet, D., McDowell, N., Vennetier, M., et al. (2010). A global overview of drought and heat-induced tree mortality reveals emerging climate change risks for forests. *For. Ecol. Manag.* 259, 660–684. doi: 10.1016/j.foreco.2009.09.001
- Allen, R. G., Pereira, L. S., Raes, D., and Smith, M. (1998). *Crop Evapotranspiration - Guidelines for Computing Crop Water Requirements - FAO Irrigation and Drainage Paper 56*. Rome: FAO - Food and Agriculture Organization of the United Nations.
- Amatya, D., and Harrison, A. (2016). Grass and forest potential evapotranspiration comparison using five methods in the Atlantic Coastal Plain. *J. Hydrol. Eng.* 21, 1–13.
- Anderegg, L. D. L., Anderegg, W. R. L., and Berry, J. A. (2013). Not all droughts are created equal: translating meteorological drought into woody plant mortality. *Tree Physiol.* 33, 672–683. doi: 10.1093/treephys/tpt044
- Anderegg, W. R. L., and Callaway, E. S. (2012). Infestation and hydraulic consequences of induced carbon starvation. *Plant Physiol.* 159, 1866–1874. doi: 10.1104/pp.112.198424
- Archambeau, J., Ruiz-Benito, P., Ratcliffe, S., Fréjaville, T., Changenet, A., Muñoz Castañeda, J. M., et al. (2020). Similar patterns of background mortality across Europe are mostly driven by drought in European beech and a combination of drought and competition in Scots pine. *Agric. For. Meteorol.* 280:107772. doi: 10.1016/j.agrformet.2019.107772
- Arend, M., Link, R. M., Patthey, R., Hoch, G., Schuldt, B., and Kahmen, A. (2021). Rapid hydraulic collapse as cause of drought-induced mortality in conifers. *Proc. Natl. Acad. Sci. U.S.A.* 118:e2025251118. doi: 10.1073/pnas.2025251118
- Babst, F., Poulter, B., Trouet, V., Tan, K., Neuwirth, B., Wilson, R., et al. (2013). Site- and species-specific responses of forest growth to climate across the European continent. *Glob. Ecol. Biogeogr.* 22, 706–717. doi: 10.1111/geb.12023
- Bachofen, C., Wohlgenuth, T., Ghazoul, J., and Moser, B. (2016). Cold temperature extremes during spring do not limit the range shift of Mediterranean pines into regions with intermittent frost. *Funct. Ecol.* 30, 856–865. doi: 10.1111/1365-2435.12581
- Badeck, F.-W., Bondeau, A., Böttcher, K., Doktor, D., Lucht, W., Schaber, J., et al. (2004). Responses of spring phenology to climate change. *New Phytol.* 162, 295–309. doi: 10.1111/j.1469-8137.2004.01059.x
- Baumgartner, A., and Reichel, E. (1975). *Die Weltwasserbilanz*. München: Oldenbourg.
- Bayazit, M., and Önöz, B. (2007). To prewhiten or not to prewhiten in trend analysis? *Hydrol. Sci. J.* 52, 611–624. doi: 10.1623/hysj.52.4.611
- Begert, M., Schlegel, T., and Kirchhofer, W. (2005). Homogeneous temperature and precipitation series of Switzerland from 1864 to 2000. *Int. J. Climatol.* 25, 65–80. doi: 10.1002/joc.1118
- Bigler, C., Bräker, O. U., Bugmann, H., Dobbertin, M., and Rigling, A. (2006). Drought as an inciting mortality factor in scots pine stands of the Valais, Switzerland. *Ecosystems* 9, 330–343. doi: 10.1007/s10021-005-0126-2
- Bose, A. K., Gessler, A., Bolte, A., Bottero, A., Buras, A., Caillet, M., et al. (2020). Growth and resilience responses of Scots pine to extreme droughts across Europe depend on predrought growth conditions. *Glob. Change Biol.* 26, 4521–4537. doi: 10.1111/gcb.15153
- Bréda, N., Huc, R., Granier, A., and Dreyer, E. (2006). Temperate forest trees and stands under severe drought: a review of ecophysiological responses, adaptation processes and long-term consequences. *Ann. For. Sci.* 63, 625–644. doi: 10.1051/forest:2006042
- Breshears, D. D., Carroll, C. J. W., Redmond, M. D., Wion, A. P., Allen, C. D., Cobb, N. S., et al. (2018). A dirty dozen ways to die: metrics and modifiers of mortality driven by drought and warming for a tree species. *Front. For. Glob. Change* 1:4. doi: 10.3389/ffgc.2018.00004
- Brodribb, T. J., and Cochard, H. (2009). Hydraulic failure defines the recovery and point of death in water-stressed conifers. *Plant Physiol.* 149, 575–584. doi: 10.1104/pp.108.129783

- Buras, A., Rammig, A., and Zang, C. S. (2020). Quantifying impacts of the 2018 drought on European ecosystems in comparison to 2003. *Biogeosciences* 17, 1655–1672. doi: 10.5194/bg-17-1655-2020
- Buras, A., Schunk, C., Zeiträg, C., Herrmann, C., Kaiser, L., Lemme, H., et al. (2018). Are Scots pine forest edges particularly prone to drought-induced mortality? *Environ. Res. Lett.* 13:025001. doi: 10.1088/1748-9326/aaa0b4
- Calanca, P., Smith, P., Holzkämper, A., and Ammann, C. (2011). Die Referenzverdunstung und ihre anwendung in der agrarmeteorologie. *Agrarforschung Schweiz* 2, 176–183.
- Camarero, J. J., Gazol, A., Sangüesa-Barreda, G., Oliva, J., and Vicente-Serrano, S. M. (2015). To die or not to die: early warnings of tree dieback in response to a severe drought. *J. Ecol.* 103, 44–57. doi: 10.1111/1365-2745.12295
- Castellví, F., Perez, P. J., Villar, J. M., and Rosell, J. I. (1996). Analysis of methods for estimating vapor pressure deficits and relative humidity. *Agric. For. Meteorol.* 82, 29–45. doi: 10.1016/0168-1923(96)02343-X
- Cech, T. L., and Perny, B. (2000). Kiefernsterben im tirol. *Forstschutz Aktuell Wien* 22, 12–15.
- CH2018 (2018). *Climate Scenarios for Switzerland, Technical Report*. Zurich: National Centre for Climate Services.
- Choat, B., Brodribb, T. J., Brodersen, C. R., Duursma, R. A., López, R., and Medlyn, B. E. (2018). Triggers of tree mortality under drought. *Nature* 558, 531–539. doi: 10.1038/s41586-018-0240-x
- Dale, V. H., Joyce, L. A., McNulty, S., Neilson, R. P., Ayres, M. P., Flannigan, M. D., et al. (2001). Climate Change and Forest Disturbances: climate change can affect forests by altering the frequency, intensity, duration, and timing of fire, drought, introduced species, insect and pathogen outbreaks, hurricanes, windstorms, ice storms, or landslides. *BioScience* 51, 723–734.
- Dobbertin, M. (2005). Tree growth as indicator of tree vitality and of tree reaction to environmental stress: a review. *Eur. J. For. Res.* 124, 319–333. doi: 10.1007/s10342-005-0085-3
- Dobbertin, M., and Brang, P. (2001). Crown defoliation improves tree mortality models. *For. Ecol. Manag.* 141, 271–284. doi: 10.1016/S0378-1127(00)00335-2
- Dobbertin, M., and Rigling, A. (2006). Pine mistletoe (*Viscum album* ssp. *austriacum*) contributes to Scots pine (*Pinus sylvestris*) mortality in the Rhone valley of Switzerland. *For. Pathol.* 36, 309–322. doi: 10.1111/j.1439-0329.2006.00457.x
- Dobbertin, M., Wermelinger, B., Bigler, C., Bürgli, M., Carron, M., Forster, B., et al. (2007). Linking increasing drought stress to Scots pine mortality and bark beetle infestations. *Sci. World J.* 7(Suppl. 1), 231–239. doi: 10.1100/tsw.2007.58
- Ducrey, M. (1998). Aspects écophysologiques de la réponse et de l'adaptation des sapins méditerranéens aux extrêmes climatiques: gelées printanières et sécheresse estivale. *For. Méditerr.* 19, 105–116.
- Dukes, J. S., Pontius, J., Orwig, D., Garnas, J. R., Rodgers, V. L., Brazee, N., et al. (2009). Responses of insect pests, pathogens, and invasive plant species to climate change in the forests of northeastern North America: what can we predict? *Can. J. For. Res.* 39, 231–248. doi: 10.1139/X08-171
- Eichhorn, J., and Roskams, P. (2013). “Chapter 8 – assessment of tree condition,” in *Developments in Environmental Science*, Vol. 12, eds M. Ferretti and R. Fischer (Amsterdam: Elsevier), 139–167. doi: 10.1186/1471-2458-11-S4-S11
- Eickenscheidt, N., and Wellbrock, N. (2014). Consistency of defoliation data of the national training courses for the forest condition survey in Germany from 1992 to 2012. *Environ. Monit. Assess.* 186, 257–275. doi: 10.1007/s10661-013-3372-3
- Eilmann, B., Zweifel, R., Buchmann, N., Graf Pannatier, E., and Rigling, A. (2011). Drought alters timing, quantity, and quality of wood formation in Scots pine. *J. Exp. Bot.* 62, 2763–2771. doi: 10.1093/jxb/erq443
- Etzold, S., Waldner, P., Thimonier, A., Schmitt, M., and Dobbertin, M. (2014). Tree growth in Swiss forests between 1995 and 2010 in relation to climate and stand conditions: recent disturbances matter. *For. Ecol. Manag.* 311, 41–55. doi: 10.1016/j.foreco.2013.05.040
- Etzold, S., Ziemnińska, K., Rohner, B., Bottero, A., Bose, A. K., Ruehr, N. K., et al. (2019). One century of forest monitoring data in Switzerland reveals species- and site-specific trends of climate-induced tree mortality. *Front. Plant Sci.* 10:307. doi: 10.3389/fpls.2019.00307
- Etzold, S., Zweifel, R., Haeni, M., Burri, S., Braun, S., Walthert, L., et al. (2018). TreeNet. Daten und Analysen der ersten fünf Messjahre. *WSL Berichte* 72, 1–70.
- Fassnacht, F. E., Latifi, H., and Koch, B. (2012). An angular vegetation index for imaging spectroscopy data—Preliminary results on forest damage detection in the Bavarian National Park, Germany. *Int. J. Appl. Earth Observ. Geoinf.* 19, 308–321. doi: 10.1016/j.jag.2012.05.018
- Ferretti, M., Nicolas, M., Bacaro, G., Brunialti, G., Calderisi, M., Croisé, L., et al. (2014). Plot-scale modelling to detect size, extent, and correlates of changes in tree defoliation in French high forests. *For. Ecol. Manag.* 311, 56–69. doi: 10.1016/j.foreco.2013.05.009
- Frei, C. (2014). Interpolation of temperature in a mountainous region using nonlinear profiles and non-Euclidean distances. *Int. J. Climatol.* 34, 1585–1605. doi: 10.1002/joc.3786
- Frei, C., and Schär, C. (1998). A precipitation climatology of the Alps from high-resolution rain-gauge observations. *Int. J. Climatol.* 18, 873–900. doi: 10.1002/(sici)1097-0088(19980630)18:8<873::aid-joc255>3.0.co;2-9
- Frei, C., and Schär, C. (2001). Detection probability of trends in rare events: theory and application to heavy precipitation in the Alpine region. *J. Clim.* 14, 1568–1584. doi: 10.1175/1520-0442(2001)014<1568:dpotir>2.0.co;2
- Frei, C., Schöll, R., Fukutome, S., Schmidli, J., and Vidale, P. L. (2006). Future change of precipitation extremes in Europe: intercomparison of scenarios from regional climate models. *J. Geophys. Res. Atmospheres* 111:D06105. doi: 10.1029/2005jd005965
- Galiano, L., Martínez-Vilalta, J., and Lloret, F. (2010). Drought-induced multifactor decline of scots pine in the pyrenees and potential vegetation change by the expansion of co-occurring Oak species. *Ecosystems* 13, 978–991. doi: 10.1007/s10021-010-9368-8
- Galiano, L., Martínez-Vilalta, J., and Lloret, F. (2011). Carbon reserves and canopy defoliation determine the recovery of Scots pine 4 yr after a drought episode. *New Phytol.* 190, 750–759. doi: 10.1111/j.1469-8137.2010.03628.x
- Gessler, A., Bächli, L., Rouholahnejad Freund, E., Treyde, K., Schaub, M., Haeni, M., et al. (2022). Drought reduces water uptake in beech from the drying topsoil, but no compensatory uptake occurs from deeper soil layers. *New Phytol.* 233, 194–206. doi: 10.1111/nph.17767
- Gessler, A., Cailleret, M., Joseph, J., Schönbeck, L., Schaub, M., Lehmann, M., et al. (2018). Drought induced tree mortality – a tree-ring isotope based conceptual model to assess mechanisms and predispositions. *New Phytol.* 219, 485–490. doi: 10.1111/nph.15154
- Giuggiola, A., Bugmann, H., Zingg, A., Dobbertin, M., and Rigling, A. (2013). Reduction of stand density increases drought resistance in xeric Scots pine forests. *For. Ecol. Manag.* 310, 827–835. doi: 10.1016/j.foreco.2013.09.030
- Gonthier, P., Giordano, L., and Nicolotti, G. (2010). Further observations on sudden diebacks of Scots pine in the European Alps. *For. Chron.* 86, 110–117. doi: 10.5558/tfc86110-1
- Grossiord, C., Buckley, T. N., Cernusak, L. A., Novick, K. A., Poulter, B., Siegwolf, R. T. W., et al. (2020). Plant responses to rising vapor pressure deficit. *New Phytol.* 226, 1550–1566. doi: 10.1111/nph.16485
- Guada, G., Camarero, J. J., Sánchez-Salguero, R., and Cerrillo, R. M. N. (2016). Limited growth recovery after drought-induced forest dieback in Very defoliated trees of two pine species. *Front. Plant Sci.* 7:418. doi: 10.3389/fpls.2016.00418
- Hargreaves, G. H., and Allen, R. G. (2003). History and evaluation of hargreaves evapotranspiration equation. *J. Irrig. Drainage Eng.* 129, 53–63. doi: 10.1061/(asce)0733-9437(2003)129:1(53)
- Hartmann, H., Moura, C. F., Anderegg, W. R. L., Ruehr, N. K., Salmon, Y., Allen, C. D., et al. (2018). Research frontiers for improving our understanding of drought-induced tree and forest mortality. *New Phytol.* 218, 15–28. doi: 10.1111/nph.15048
- Haylock, M. R., Hofstra, N., Klein Tank, A. M. G., Klok, E. J., Jones, P. D., and New, M. (2008). A European daily high-resolution gridded data set of surface temperature and precipitation for 1950–2006. *J. Geophys. Res. Atmospheres* 113:D20119. doi: 10.1029/2008JD010201
- Holst, J., Barnard, R., Brandes, E., Buchmann, N., Gessler, A., and Jaeger, L. (2008). Impacts of summer water limitation on the carbon balance of a Scots pine forest in the southern upper Rhine plain. *Agric. For. Meteorol.* 148, 1815–1826. doi: 10.1016/j.agrformet.2008.06.008
- Innes, J. L. (1995). Theoretical and practical criteria for the selection of ecosystem monitoring plots in Swiss forests. *Environ. Monit. Assess.* 36, 271–294. doi: 10.1007/BF00547906
- Innes, J. L. (1998). An assessment of the use of crown structure for the determination of the health of beech (*Fagus sylvatica*). *For. Int. J. For. Res.* 71, 113–130. doi: 10.1093/forestry/71.2.113

- IPCC (2014). *Climate Change 2014: Synthesis Report. Contribution of Working Groups I, II and III to the Fifth Assessment Report of the Intergovernmental Panel on Climate Change*. Geneva: IPCC.
- Jaime, L., Batllori, E., Margalef-Marrase, J., Pérez Navarro, M. Á, and Lloret, F. (2019). Scots pine (*Pinus sylvestris* L.) mortality is explained by the climatic suitability of both host tree and bark beetle populations. *For. Ecol. Manag.* 448, 119–129. doi: 10.1016/j.foreco.2019.05.070
- Joseph, J., Gao, D., Backes, B., Bloch, C., Brunner, I., Gleixner, G., et al. (2020). Rhizosphere activity in an old-growth forest reacts rapidly to changes in soil moisture and shapes whole-tree carbon allocation. *Proc. Natl. Acad. Sci. U.S.A.* 117, 24885–24892. doi: 10.1073/pnas.2014084117
- Kellomaki, S., Hanninen, H., and Kolstrom, M. (1995). Computations on frost damage to scots pine under climatic warming in boreal conditions. *Ecol. Appl.* 5, 42–52. doi: 10.2307/1942050
- Kendall, M. G. (1948). *Rank Correlation Methods*. London: Griffin.
- MacAllister, S., Mencuccini, M., Sommer, U., Engel, J., Hudson, A., Salmon, Y., et al. (2019). Drought-induced mortality in Scots pine: opening the metabolic black box. *Tree Physiol.* 39, 1358–1370. doi: 10.1093/treephys/tpz049
- Madrigal-González, J., Herrero, A., Ruiz-Benito, P., and Zavala, M. A. (2017). Resilience to drought in a dry forest: insights from demographic rates. *For. Ecol. Manag.* 389, 167–175. doi: 10.1016/j.foreco.2016.12.012
- Manion, P. D. (1991). *Tree Disease Concepts*. Englewood Cliffs, NJ: Prentice Hall.
- Mann, H. B. (1945). Nonparametric tests against trend. *Econometrica* 13, 245–259. doi: 10.2307/1907187
- Martin-Benito, D., Anchukaitis, K. J., Evans, M. N., Del Río, M., Beekman, H., and Cañellas, I. (2017). Effects of drought on xylem anatomy and water-use efficiency of two co-occurring pine species. *Forests* 8:332. doi: 10.3390/f8090332
- Martin-Benito, D., Beekman, H., and Cañellas, I. (2013). Influence of drought on tree rings and tracheid features of *Pinus nigra* and *Pinus sylvestris* in a mesic Mediterranean forest. *Eur. J. For. Res.* 132, 33–45. doi: 10.1007/s10342-012-0652-3
- Masaitis, G., Mozgeris, G., and Augustaitis, A. (2013). Spectral reflectance properties of healthy and stressed coniferous trees. [Spectral reflectance properties of healthy and stressed coniferous trees]. *iForest Biogeosci. For.* 6, 30–36. doi: 10.3832/ifer0709-006
- McDowell, N., Pockman, W. T., Allen, C. D., Breshears, D. D., Cobb, N., Kolb, T., et al. (2008). Mechanisms of plant survival and mortality during drought: why do some plants survive while others succumb to drought? *New Phytol.* 178, 719–739. doi: 10.1111/j.1469-8137.2008.02436.x
- McMahon, T. A., Peel, M. C., Lowe, L., Srikanthan, R., and McVicar, T. R. (2013). Estimating actual, potential, reference crop and pan evaporation using standard meteorological data: a pragmatic synthesis. *Hydrol. Earth Syst. Sci.* 17, 1331–1363. doi: 10.5194/hess-17-1331-2013
- Minerbi, S., Cescatti, A., Cherubini, P., Hellrigl, K., Markart, G., Saurer, M., et al. (2006). La siccità dell'estate 2003 causa di disseccamenti del pino silvestre in Val d'Isarco. *For. Obs.* 2, 89–144.
- Monteith, J. L. (1965). "Evaporation and environment. The state and movement of water in living organisms," in *Proceedings of the 19th Symposium of the Society for Experimental Biology*, Vol. 19, (New York, NY: Academic Press), 205–234.
- Ortega-Farías, S., Irmak, S., and Cuenca, R. H. (2009). Special issue on evapotranspiration measurement and modeling. *Irrig. Sci.* 28, 1–3. doi: 10.1007/s00271-009-0184-x
- Park Williams, A., Allen, C. D., Macalady, A. K., Griffin, D., Woodhouse, C. A., Meko, D. M., et al. (2013). Temperature as a potent driver of regional forest drought stress and tree mortality. *Nat. Clim. Change* 3, 292–297. doi: 10.1038/nclimate1693
- Pastirčáková, K., Adamčíková, K., Pastirčák, M., Zach, P., Galko, J., Kovčè, M., et al. (2018). Two blue-stain fungi colonizing Scots pine (*Pinus sylvestris*) trees infested by bark beetles in Slovakia, Central Europe. *Biologia* 73, 1053–1066. doi: 10.2478/s11756-018-0114-6
- Penman, H. L. (1948). Natural evaporation from open water, bare soil and grass. *Proc. R. Soc. Lond. Ser. Math. Phys. Sci.* 193, 120–145. doi: 10.1098/rspa.1948.0037
- Pfister, A., Krehan, H., Perny, B., Tomiczek, C., Buchberger, A., and Lick, H. (2001). *Kiefernsschäden – Erkennen und Vermeiden*. Wien: Merkblatt Amt der Steyermärkischen Landesregierung, Fachabteilung Forstwesen und Forstliche Bundesversuchsanstalt.
- Rebetez, M., and Dobbertin, M. (2004). Climate change may already threaten Scots pine stands in the Swiss Alps. *Theor. Appl. Climatol.* 79, 1–9. doi: 10.1007/s00704-004-0058-3
- Reid, P. C., Hari, R. E., Beaugrand, G., Livingstone, D. M., Marty, C., Straile, D., et al. (2016). Global impacts of the 1980s regime shift. *Glob. Change Biol.* 22, 682–703. doi: 10.1111/gcb.13106
- Rigling, A., and Cherubini, P. (1999). What is the cause of the high mortality rates of the Scots pines in the «Telwald» near Visp (Switzerland)? A summary of previous studies and a dendroecological study. *Schweiz. Z. Forstwesen* 150, 113–131. doi: 10.3188/szf.1999.0113
- Rigling, A., Bigler, C., Eilmann, B., Feldmeyer-Christe, E., Gimmi, U., Ginzler, C., et al. (2013). Driving factors of a vegetation shift from Scots pine to pubescent oak in dry Alpine forests. *Glob. Change Biol.* 19, 229–240. doi: 10.1111/gcb.12038
- Rigling, A., Dobbertin, M., Bürgi, M., Gimmi, U., Graf Pannatier, E., Gugerli, F., et al. (2006). *Verdrängen Flaumeichen die Walliser Waldföhren? Merkblatt für die Praxis*, Vol. 41. Birmensdorf: Eidg. Forschungsanstalt WSL.
- Rigling, A., Moser, B., Feichtinger, L., Gärtner, H., Giugliola, A., Hug, C., et al. (2018). 20 Jahre waldföhrensterben im Wallis: rückblick und aktuelle Resultate. *Schweiz. Z. Forstwesen* 169, 242–250. doi: 10.3188/szf.2018.0242
- Rood, S. B., Patiño, S., Coombs, K., and Tyree, M. T. (2000). Branch sacrifice: cavitation-associated drought adaptation of riparian cottonwoods. *Trees* 14, 248–257. doi: 10.1007/s004680050010
- Schönbeck, L., Gessler, A., Hoch, G., McDowell, N. G., Rigling, A., Schaub, M., et al. (2018). Homeostatic levels of nonstructural carbohydrates after 13 yr of drought and irrigation in *Pinus sylvestris*. *New Phytol.* 219, 1314–1324. doi: 10.1111/nph.15224
- Schuld, B., Buras, A., Arend, M., Vitasse, Y., Beierkuhnlein, C., Damm, A., et al. (2020). A first assessment of the impact of the extreme 2018 summer drought on Central European forests. *Basic Appl. Ecol.* 45, 86–103. doi: 10.1016/j.baae.2020.04.003
- Seager, R., Hooks, A., Williams, A. P., Cook, B., Nakamura, J., and Henderson, N. (2015). Climatology, variability, and trends in the U.S. Vapor Pressure Deficit, an important fire-related meteorological quantity. *J. Appl. Meteorol. Climatol.* 54, 1121–1141. doi: 10.1175/jamc-d-14-0321.1
- Sen, P. K. (1968). Estimates of the regression coefficient based on Kendall's Tau. *J. Am. Stat. Assoc.* 63, 1379–1389. doi: 10.2307/2285891
- Senf, C., Buras, A., Zang, C. S., Rammig, A., and Seidl, R. (2020). Excess forest mortality is consistently linked to drought across Europe. *Nat. Commun.* 11:6200. doi: 10.1038/s41467-020-19924-1
- Sentelhas, P. C., Gillespie, T. J., and Santos, E. A. (2010). Evaluation of FAO Penman–Monteith and alternative methods for estimating reference evapotranspiration with missing data in Southern Ontario, Canada. *Agric. Water Manag.* 97, 635–644. doi: 10.1016/j.agwat.2009.12.001
- Sidor, C. G., Camarero, J. J., Popa, I., Badea, O., Apostol, E. N., and Vlad, R. (2019). Forest vulnerability to extreme climatic events in Romanian Scots pine forests. *Sci. Total Environ.* 678, 721–727. doi: 10.1016/j.scitotenv.2019.05.021
- Skelton, R. P., Brodribb, T. J., McAdam, S. A. M., and Mitchell, P. J. (2017). Gas exchange recovery following natural drought is rapid unless limited by loss of leaf hydraulic conductance: evidence from an evergreen woodland. *New Phytol.* 215, 1399–1412. doi: 10.1111/nph.14652
- Sumner, D. M., and Jacobs, J. M. (2005). Utility of Penman–Monteith, Priestley–Taylor, reference evapotranspiration, and pan evaporation methods to estimate pasture evapotranspiration. *J. Hydrol.* 308, 81–104. doi: 10.1016/j.jhydrol.2004.10.023
- Taccoen, A., Piedallu, C., Seynave, I., Perez, V., Gégout-Petit, A., Nageleisen, L.-M., et al. (2019). Background mortality drivers of European tree species: climate change matters. *Proc. R. Soc. B Biol. Sci.* 286:20190386. doi: 10.1098/rspb.2019.0386
- Teskey, R., Wertin, T., Bauweraers, I., Ameye, M., McGuire, M. A., and Steppe, K. (2015). Responses of tree species to heat waves and extreme heat events. *Plant Cell Environ.* 38, 1699–1712. doi: 10.1111/pce.12417
- Theil, H. (1950). A rank-invariant method of linear and polynomial regression analysis. *Indag. Math.* 12, 85–91, 173–177, 1967–1982.
- Timofeeva, G., Treyde, K., Bugmann, H., Rigling, A., Schaub, M., Siegwolf, R., et al. (2017). Long-term effects of drought on tree-ring growth and carbon isotope variability in Scots pine in a dry environment. *Tree Physiol.* 8, 1028–1041. doi: 10.1093/treephys/tpx041

- Trotsiuk, V., Hartig, F., Cailleret, M., Babst, F., Forrester, D. I., Baltensweiler, A., et al. (2020). Assessing the response of forest productivity to climate extremes in Switzerland using model–data fusion. *Glob. Chang. Biol.* 26, 2463–2476. doi: 10.1111/gcb.15011
- Vacchiano, G., Garbarino, M., Borgogno Mondino, E., and Motta, R. (2012). Evidences of drought stress as a predisposing factor to Scots pine decline in Valle d'Aosta (Italy). *Eur. J. For. Res.* 131, 989–1000. doi: 10.1007/s10342-011-0570-9
- Vilà-Cabrera, A., Martínez-Vilalta, J., Galiano, L., and Retana, J. (2013). Patterns of forest decline and regeneration across scots pine populations. *Ecosystems* 16, 323–335. doi: 10.1007/S10021-012-9615-2
- Vitasse, Y., and Rebetez, M. (2018). Unprecedented risk of spring frost damage in Switzerland and Germany in 2017. *Clim. Change* 149, 233–246. doi: 10.1007/s10584-018-2234-y
- Vitasse, Y., Schneider, L., Rixen, C., Christen, D., and Rebetez, M. (2018). Increase in the risk of exposure of forest and fruit trees to spring frosts at higher elevations in Switzerland over the last four decades. *Agric. For. Meteorol.* 248, 60–69. doi: 10.1016/j.agrformet.2017.09.005
- Wang, X. L., and Swail, V. R. (2001). Changes of extreme wave heights in Northern Hemisphere oceans and related atmospheric circulation regimes. *J. Clim.* 14, 2204–2221. doi: 10.1175/1520-0442(2001)014<2204:coewhi>2.0.co;2
- Weber, P., Bugmann, H., and Rigling, A. (2007). Radial growth responses to drought of *Pinus sylvestris* and *Quercus pubescens* in an inner-Alpine dry valley. *J. Veg. Sci.* 18, 777–792. doi: 10.1111/j.1654-1103.2007.tb02594.x
- Wermelinger, B., Rigling, A., Schneider Mathis, D., and Dobbertin, M. (2008). Assessing the role of bark- and wood-boring insects in the decline of Scots pine (*Pinus sylvestris*) in the Swiss Rhone valley. *Ecol. Entomol.* 33, 239–249. doi: 10.1111/j.1365-2311.2007.00960.x
- Zhang, X., and Zwiers, F. W. (2004). Comment on “Applicability of prewhitening to eliminate the influence of serial correlation on the Mann-Kendall test” by Sheng Yue and Chun Yuan Wang. *Water Resour. Res.* 40:5. doi: 10.1029/2003WR002073
- Zohner, C. M., Mo, L., Renner, S. S., Svenning, J.-C., Vitasse, Y., Benito, B. M., et al. (2020). Late-spring frost risk between 1959 and 2017 decreased in North America but increased in Europe and Asia. *Proc. Natl. Acad. Sci. U.S.A.* 117, 12192–12200. doi: 10.1073/pnas.1920816117
- Zweifel, R., Bangerter, S., Rigling, A., and Sterck, F. J. (2012). Pine and mistletoes: how to live with a leak in the water flow and storage system? *J. Exp. Bot.* 63, 2565–2578. doi: 10.1093/jxb/err432
- Zweifel, R., Etzold, S., Sterck, F., Gessler, A., Anfodillo, T., Mencuccini, M., et al. (2020). Determinants of legacy effects in pine trees – implications from an irrigation-stop experiment. *New Phytol.* 227, 1081–1096. doi: 10.1111/nph.16582
- Zweifel, R., Haeni, M., Buchmann, N., and Eugster, W. (2016). Are trees able to grow in periods of stem shrinkage? *New Phytol.* 211, 839–849. doi: 10.1111/nph.13995
- Zweifel, R., Sterck, F., Braun, S., Buchmann, N., Eugster, W., Gessler, A., et al. (2021). Why trees grow at night. *New Phytol.* 231, 2174–2185. doi: 10.1111/nph.17552

Conflict of Interest: The authors declare that the research was conducted in the absence of any commercial or financial relationships that could be construed as a potential conflict of interest.

Publisher's Note: All claims expressed in this article are solely those of the authors and do not necessarily represent those of their affiliated organizations, or those of the publisher, the editors and the reviewers. Any product that may be evaluated in this article, or claim that may be made by its manufacturer, is not guaranteed or endorsed by the publisher.

Copyright © 2022 Hunziker, Begert, Scherrer, Rigling and Gessler. This is an open-access article distributed under the terms of the Creative Commons Attribution License (CC BY). The use, distribution or reproduction in other forums is permitted, provided the original author(s) and the copyright owner(s) are credited and that the original publication in this journal is cited, in accordance with accepted academic practice. No use, distribution or reproduction is permitted which does not comply with these terms.